5-15-2015

Using the Sulfur Cycle to Constrain Changes in Seawater Chemistry During the Paleogene

Kara Elizabeth Dennis
Syracuse University

Abstract

The sulfur isotopic composition of seawater sulfate ($\delta^{34}S$) has varied significantly throughout the Phanerozoic and is related to variability in Earth's sulfur and carbon cycles. During the Early Eocene (~55 Ma to 45 Ma) the $\delta^{34}S$ composition of seawater sulfate increased from +18‰ to +22‰ and has remained largely invariant over the last 34 Ma. The two principal hypotheses invoked to explain this positive excursion are: (1) a rapid increase in the flux of weathering-derived sulfate and an increase in sulfate concentrations, coupled with a compensatory increase in pyrite burial, or (2) an increase in the pyrite burial flux due to an expansion in the volume of anoxic waters. A clear understanding of this significant change in seawater sulfate chemistry is hampered by the relatively low temporal sampling resolution of data that reflect seawater sulfate $\delta^{34}S$ during this period, and potential problems with the preservation of primary signals. Here, we use $\delta^{34}S$ analysis of carbonate associated sulfate (CAS) from IODP Expedition 342, Newfoundland Drifts to test the pattern observed in marine barite $\delta^{34}S$ records (Paytan et al., 1998) and to increase the temporal resolution of the $\delta^{34}S$ isotope curve through the Eocene excursion. Despite the broad variability in the CAS record, these new data largely confirm the magnitude and timing of change observed in the Paytan et al. (1998) marine barite $\delta^{34}S$ records, but the magnitude of the excursion is higher in the CAS record. Additionally, we observe a series of anomalous $\delta^{34}S$ values that appear to the result from oxidation of ^{34}S-depleted pyrite during CAS extraction or incorporation of ^{34}S-enriched sulfate during authigenesis. These depleted or enriched values in the CAS record correlate with a lower concentration of CAS, suggesting that such samples are more susceptible to contamination of non-CAS sulfur during either extraction or original precipitation. We also performed $\delta^{34}S$

analyses on pore-water sulfate to better constrain possible influences from pore-water sulfate on CAS $\delta^{34}S$. These pore-water sulfate data indicate that microbial sulfate reduction is ongoing at sub-seafloor depths, yielding enriched pore-water sulfate values with depth. But, we observe no strong correlation between pore-water and CAS $\delta^{34}S$, suggesting that pore water sulfate contamination may not be the mechanism causing enriched CAS $\delta^{34}S$ values. Our data do not provide a clear consensus between the two proposed mechanisms for this excursion, weathering-derived sulfate or an increase volume of anoxic waters; a surge in volcanically derived sulfur associated with sea-floor spreading offers an alternative mechanism for generating this positive excursion.

USING THE SULFUR CYCLE TO CONSTRAIN CHANGES IN SEAWATER CHEMISTRY DURING THE PALEOGENE

by

Kara Dennis

B.A., Macalester College, St. Paul, MN 2012

THESIS

Submitted in partial fulfillment of the requirements for the degree of Master of Science in Earth Sciences in the Graduate School of Syracuse University

Syracuse University 2015

May 2015

Acknowledgements

Thanks to my MS advisor, Dr. Christopher Junium, for taking a chance on me. Dr. Junium gave me financial support and helped plan a great research project for me while also juggling be a new faculty member, having a lab under construction, and having a young family. I also want to thank my committee members, Dr. Linda Ivany and Dr. Scott Samson, your classes and guidance, which were an essential part of my graduate school career. Dr. Daniel Curewitz thanks for all of your guidance and advice. A special thanks to the lovely ladies in the office, you are like other-mothers to me. I am really appreciative to this department and all of the amazing friendships that I have formed during my time at Syracuse University. I am beyond grateful for my wonderful family and my partner in crime, Ross Salerno, who have patiently listening to me excessively talking about my project for the past two years.

Table of Contents

List of Figures

Introduction

The sulfur cycle is intimately linked to the carbon and oxygen cycles and reflects changes in the redox state of the ocean, the size of the oceanic sulfate reservoir, weathering and ocean circulation. Sulfate is the third most prevalent constituent of modern seawater, and sulfur is integral to many biogeochemical reactions that affect the global marine carbon and oxygen cycles (Paytan and Gray, 2012). Sulfur holds the majority of the oxidative power of the deep ocean through microbial sulfate reduction (MSR), the principal mechanism for the oxidation of organic matter in marine sediments (Paytan and Gray, 2012; Kasten and Jørgensen, 2000). The isotopic record of seawater sulfate ($\delta^{34}S$) tracks these climate and tectonic changes through changes in the fluxes to the marine sulfate reservoir.

During the pinnacle of the Early Eocene greenhouse (~60 Ma to 48 Ma), the sulfur isotope composition of sulfate ($\delta^{34}S$) in the ocean increased dramatically from +18‰ to +22‰ (Paytan et al, 1998; Wortmann and Paytan, 2012). This is one of largest and most rapid changes in the sulfur isotope record during the last 120 Ma (*Figure 1*). The principal hypotheses used to explain this excursion invoke expanded oceanic anoxia and pyrite burial (Kurtz et al., 2003), or a rapid increase in the flux of weathering-derived sulfate (Wortmann and Paytan, 2012). However, the evidence in the geologic record for either hypothesis is equivocal, and both mechanisms may impart the same signal on the sulfur isotopic composition of seawater sulfate. A clear understanding of this change in seawater chemistry is, in part, hampered by the low temporal resolution of the $\delta^{34}S$ record during this 12 Ma period which is constrained by only 10 data points from widely distributed sites using the marine barite proxy for $\delta^{34}S$.

The primary focus of this project is two-fold, we develop a higher resolution $\delta^{34}S$ record through this interval of time using carbonate-associated sulfate (CAS) of bulk carbonates from cores extracted from the Newfoundland Drifts during Integrated Ocean Drilling Program (IODP) Expedition (EXP) 342. This locality had very high sedimentation rates during the interval of interest (Norris et al., 2014), and allows for high-resolution study. The carbonates recovered from the drift intervals of the EXP 342 sites are well preserved as indicated by the presence of glassy foraminfera (Norris et al., 2014). Second, we assess the fidelity of the CAS record and the degree to which it can reproduce the Paytan et al. (1998) marine barite $\delta^{34}S$ record. The CAS proxy is widely used in deep-time sulfur cycle studies (Rennie and Turchyn, 2014) and is a more attractive target for sulfur isotope studies than marine barite because of the ubiquity of carbonates in the geologic record. This study serves as an important comparison of the two proxies, barite and CAS $\delta^{34}S$. Lastly, this study also allows for an exploration of sources for the frequently observed variability in CAS data. This noise is often attributed to true variability in the sulfur cycle during intervals of time when the size of the sulfate reservoir was likely smaller and more sensitive to change than today, such as the Neoproterozoic and before the Great Oxidation Event. Some studies, however, speculate that pore-water sulfate contamination could be the cause of variability in CAS data (Turchyn et al. 2009) because microbial sulfate reduction (MSR) causes significant fractionation in sulfur isotopes in the sediment pore-water system. Comparison of our bulk carbonate $\delta^{34}S$ CAS record to the $\delta^{34}S$ profile of pore-water sulfate provides an important control on the integrity of the CAS proxy.

Background

Modern Sulfur Cycle

Seawater sulfate is the product of oxidative weathering of sedimentary sulfides and the dissolution of evaporite deposits delivered via river input (*Figure 2*) (Rees et al., 1978; Raab and Spiro, 1991; Thode and Monster, 1961). Volcanic outgassing of SO_2 from hydrothermal vents serves as another source of sulfur into the Earth's surface reservoirs (Arthur, 2000). The principal sinks for seawater sulfate are MSR and the precipitation/burial of sulfate evaporite minerals (Thode and Monster, 1961; Raab and Spiro, 1991).

Seawater sulfate makes up ~13% of the total inventory of sulfur compounds on the Earth's surface (Schlesinger, 1997). The modern ocean has ~1.3×10^{21} g of sulfur, and a significant sink for seawater sulfate is MSR, which reduces ~30×10^{13} g of sulfur a year (Turchyn and Shrag, 2004; Bottrell and Newton, 2006; Walker, 1986) (*Figure 2*). About 75-90% of sulfur reduced by MSR, gets re-oxidized and the remainder of the reduced sulfur from MSR, ~20%, is typically buried as pyrite and other metal sulfides (~6×10^{13} g of sulfur a year). A small fraction of sulfur is buried during the precipitation of carbonates as CAS, ~0.58×10^{13} g a year (Strauss, 1999). Locally, MSR rates are primarily dependent on the quantity of organic material, even when sulfate availability is low (Kao et al., 2004). Given that availability of organic substrates is spatially and temporally heterogeneous, MSR rates are also highly variable within marine environments (Bowles et al., 2014). The balance of these processes, particularly the relative proportions of seawater sulfate and sulfide minerals buried as pyrite can be estimated using sulfur isotopes.

Sulfur Isotope Systematics

The primary tool for tracking changes in the sulfur cycle is measuring the stable isotopes of sulfur in sedimentary phases. There are four stable isotopes of sulfur (in order of abundance), ^{32}S (95.02%), ^{34}S(4.21%), ^{33}S (0.75%), and ^{36}S (0.02%) (Wieser, 2006). MSR preferentially dissimilates sulfate with the lighter sulfur isotope (^{32}S). This causes a significant fractionation between the seawater sulfate reservoir and sulfide minerals/pyrite in marine sediments that results in ^{34}S-depleted sulfide minerals. The most significant and prevalent isotopic fractionation in the sulfur cycle is driven by MSR (Ault and Kulp, 1959; Thode and Monster, 1961) and ultimate sequestration of that sulfate during the burial of pyrite.

The isotopic ratio of sulfur is typically measured between the two most abundant isotopes. The ratio measurements of ^{34}S:^{32}S are expressed as a $\delta^{34}S$ values. The ^{34}S:^{32}S ratio within a sample is measured against the known ratio from an international reference standard. The standard for sulfur isotope work is Canyon Diablo Troilite (CDT), a meteorite from Meteor Crater, AZ (Ault and Jensen, 1963). CDT, like that of volcanically derived sulfur (sulfide or SO_2), has an isotopic ratio of 0‰, since biologic fractionation is not pertinent in these environments of origin. Increasingly positive $\delta^{34}S$ values indicate a higher abundance of the ^{34}S isotope relative to the international standard. The $\delta^{34}S$ value of modern seawater is about 21.0‰ (Rees et al., 1978). The $\delta^{34}S$ value of pyrite/sulfide minerals varies, although values are typically depleted relative to seawater sulfate. On the basis of laboratory experiments, pyrite values can vary between +4 to -70‰ in relation to seawater sulfate (Strauss, 1999; Canfield et al., 2010), but some studies indicate that MSR fractionation can be less dramatic in low sulfate conditions (Kah et al., 2004; Habicht et al., 2002; Canfield and Teske, 1996).

Ault and Kulp (1959) found that the $\delta^{34}S$ composition of seawater sulfate was essentially homogenous. This is the result of the long residence time of sulfate in the ocean, ~13-20 Ma (Claypool et al., 1980; Paytan et al., 2004). Therefore, seawater sulfate is very well mixed, and the data from a series of cores from one particular region are assumed to be reasonably representative of global sulfate $\delta^{34}S$. This assumption only holds as long as the reservoir size is large and the residence time is significantly longer than oceanic mixing times. Careful analysis of the marine sulfur isotope record can provide information on the fraction of sulfur buried as pyrite, the rates of evaporite and sulfide weathering, the concentrations of seawater sulfate in the marine reservoir, and a more complete understanding of global marine redox conditions (e.g. Kurtz et al., 2003).

Microbial Sulfate Reduction (MSR)

The supply of oxygen to marine sediments is normally limited to the top few cm because aerobic respiration rapidly consumes the available supply of oxygen. Since sulfate is so abundant in seawater and prevalent in seafloor sediments via diffusion, it serves as the primary electron acceptor in anaerobic degradation of organic material in the marine sediments via microbial sulfate reduction (Henrichs and Reeburgh, 1987). During MSR sulfate (SO_4^{2-}) is reduced to hydrogen sulfide (H_2S) using an electron donor such as acetate, methane, or more complex organic molecules (see equation below).

Basic MSR Equation: $\mathbf{SO_4^{2-} + 2CH_2O \rightarrow H_2S + 2HCO_3^-}$

The resulting hydrogen sulfide can react with soluble chalchophile metals such as Fe^{2+} or Ni^{2+} to form sulfide minerals such as pyrite (FeS_2) (Thode and Monster, 1961). The hydrogen sulfide can also diffuse out of sediments and be re-oxidized, returning it to the seawater sulfate

reservoir. MSR is therefore dependent on the presence of an electron donor such as organic matter, and the extent of this process is mechanistically linked to the burial of organic matter. This relationship is clearly revealed in the high concentrations of pyrite in organic matter-rich sediments and the lack of pore water sulfate in these settings. This relationship also provides the basis for the correspondence between the $\delta^{34}S$ of sedimentary phases and the $\delta^{13}C$ of carbonates and organic carbon through time in that both proxies follow the relative burial flux of the reduced phase (Kurtz et al., 2003).

A secondary effect of sulfate reduction is the release of phosphorus during organic matter degradation, one of the principal limiting nutrients for primary productivity (*Figure 3*) (Adams et al., 2010; Caraco et al., 1993). MSR is one of the most ancient metabolic processes and has been a dominant biogeochemical mechanism influencing the chemistry of Earth's surface for the past 2.75 billion years (Canfield et al., 2000). A better understanding of changes in the sulfur cycle can provide perspective for determining the biotic response and implications of variability in the concentration of sulfate through time.

Seawater Sulfate in the Geologic Record

Sulfate concentrations and residence times have generally increased over Earth history as the ocean-atmosphere system has become more oxidized (Kah et al., 2004; Canfield, 2004). Thus, the sensitivity of the sulfate reservoir to isotopic change has changed as the concentration of sulfate has increased as well as the fractionation between the oxidized and reduced reservoirs (*Figure 3*). Studies on the $\delta^{34}S$ isotope record of Proterozoic carbonates show significant variability, which is attribute to a small sulfate reservoir in a world with lower concentrations of atmospheric oxygen (Hurtgen et al., 2002; Kah et al., 2004).

Though the Phanerozoic is thought to have had relatively stable atmospheric oxygen levels, variability within the marine sulfate cycle has persisted into the Cenozoic Era (*Figure 4, 5, & 6*) (Claypool et al., 1980, Kampschulte and Strauss, 2004; Paytan et al, 1998). This Phanerozoic variability in the $\delta^{34}S$-record is attributed to changes in major sulfur fluxes into and out of the marine sulfate reservoir. These fluxes may be the result of changes in the marine evaporite reservoir or changes in ocean circulation and redox state, leading to variability in MSR (Bottrell and Newton, 2006; Hay et al., 2006).

Evaporite Studies

Claypool et al. (1980) produced the first long-term $\delta^{34}S$ isotope record from marine evaporites, which captures the $\delta^{34}S$ of the seawater at the time of evaporite precipitation (*Figure 4*). Evaporite precipitation involves a relatively minimal fractionation of ~+0.3-2.4‰ from seawater (Thode and Monster, 1961). This "Claypool Curve" (1980) suggested that the fluxes of sulfur into and out of the ocean might have been quite variable during the Precambrian and well into the Phanerozoic. This plasticity in the sulfur cycle through geologic time warrants a further study, but evaporites are difficult to date, easily eroded, and not continuous throughout the geologic record. Additionally, Raab and Spiro (1991) found that the $\delta^{34}S$ values of evaporites can vary with progressive fractional crystallization, which could limit the validity of evaporates as a proxy for seawater sulfate.

Marine Barite Studies

Paytan et al. (1998) produced a $\delta^{34}S$ Cenozoic record of seawater sulfate from biogenic barite (Gonzalez-Munoz et al., 2012), which has a minimal fractionation from seawater. This alternate proxy produced higher resolution records of the $\delta^{34}S$ of seawater sulfate and provide

further evidence for the elasticity of the marine sulfate cycle in the Phanerozoic (Paytan et al, 1998) (*Figures 1*). Although a fairly complete $\delta^{34}S$ record has been attained using marine barite (Paytan et al., 1998 and 2004), marine barite studies are very difficult to undertake. There are multiple origins for marine barite, such as diagenetic and hydrothermal barite. Authigenic marine barite, which precipitates directly from the water column (Gonzalez-Munoz et al., 2012), is typically in low concentration and it is difficult to differentiate from the many other types of marine barite (Paytan et al., 2002; Griffith and Paytan, 2012). Additionally, marine barites become increasing more difficult to find in sediments older than the Cenozoic. Careful consideration of crystal morphology, size and shape via SEM imaging as well as Sr and S isotope characterization is necessary to identify candidates suitable for $\delta^{34}S$ isotopic analyses (Paytan et al., 2002).

Carbonate Associated Sulfate Studies

Kaplan et al. (1963) found trace amounts of sulfate incorporated in the biogenic calcite of mollusk shells. Busenberg and Plummer (1984) discovered that, under laboratory synthesis, seawater sulfate concentrations positively correlate with the concentration of carbonate-associated sulfate (CAS). Burdett et al. (1989) established that in Neogene biogenic carbonates the sulfur isotope composition of CAS accurately records that of marine sulfate and is unaffected by burial. This established CAS as a proxy for determining paleo-seawater sulfate isotope compositions (Burdette et al., 1989). Although CAS is present in carbonates, it is a very minor constituent. The modern ocean has ~$1.3x10^{21}$ g of sulfur, and only ~$0.58x10^{13}$ g of sulfur a year get incorporated as CAS (Strauss, 1999). Kump and Arthur (1999) calculated that about $0.5x10^{15}$ g of carbon are precipitated as $CaCO_3$ in marine carbonate sediments every year in the modern ocean. This suggests a ~0.12% CAS content in modern carbonates. Pigitore et al. (1995)

estimated a maximum of 0.5% CAS in biogenic carbonates and 0.6% CAS in diagenetic carbonates. Since carbonate sequences are abundant in the Geologic record, CAS studies have the potential to create high-resolution $\delta^{34}S$ records.

Geologic Setting

IODP Sites U1407, U1408, U1409, and U1410 were all located on the slopes of seamounts on the South East Newfoundland Ridge and proximal to the remains of the HMS Titanic. These sites were well above the Paleogene CCD but close enough to detect changes in carbon cycling during the Paleogene and alterations to the paleo-CCD during the Eocene greenhouse climate (Norris et al., 2014). This area was targeted for drilling because of the presence of plastered drift deposits that are clay-rich and are known to preserve foraminferal carbonate to a degree that is highly suitable for paleoceanographic studies. These plastered drifts accumulated on the slopes of seamounts on the northeastern or southwestern sides of seamounts (Figure 7). These drifts also have very high accumulation rates (~1-2 cm/k.y.), which makes these sediments suitable for high-resolution paleoceanographic studies (Norris et al., 2014).

Materials

IODP and ODP Samples

Core sample materials were collected during IODP Expedition 342, Newfoundland Drifts, located in the Central North Atlantic Ocean (*Figure 7*). The principal lithology for selected samples was a high carbonate content, and the source of this carbonate was primarily from foraminferal and nannofossil ooze (Norris et al., 2014), sediments with high carbonate content. Selected 'squeeze cake' samples are the residual solid sediment following pressing of

samples for the acquisition of pore waters for shipboard geochemical analyses. These samples are advantageous because of their large size and are accompanying wide range of inorganic geochemical analyses. We selected 4 squeeze cake samples from site U1410A, 10 samples from U1409A, 11 samples from U1408A, and 7 samples from U1407A. These sites were considered ideal for bulk CAS extraction because they were above the CCD and had high sedimentation rates for open ocean settings (1-3 cm/k.y.) (Norris et al., 2014). Collectively, these samples span an interval of time between 35 to 65 Ma and had a elevated carbonate content relative to the other sites targeted during the expedition. Additionally, for a higher resolution between 50 to 45 Ma, We utilized 11 core samples from Sites U1407A and U1407B. To better constrain possible diagenetic implications of microbial sulfate reduction with depth, We used complimentary pore-water fluids from the squeeze-cake samples at site U1409 to analyze the sulfur isotopic composition of the pore-water sulfate. We also selected 6 samples from ODP expedition 207 sites 1258, 1260, 1261, and 1257 to compare isotopic values from a different locality and using carbonate material that was considered less well preserved (Erbacher et al., 2004) (*Figure 8*).

Methods

CAS Extraction

The CAS extraction procedure that we utilized is modified from Burdett et al. (1989) and Gill et al. (2007). Powdered samples (30-60g) were soaked in 10% sodium chloride (NaCl) solution for two 12-hour rinses for the purpose of removing any elemental sulfur compounds or pore-water sulfate. NaCl soaked samples were rinsed in deionized water (DI) and filtered for 3 twelve-hour rinses. Multiple leaching steps are necessary to remove the non-CAS sulfur (Wotte et al., 2012). These soluble sulfates will react with NaCl to form Na_2SO_4 and $BaCl_2$. Additional

rinses were performed if sulfate remained after testing the rinse water by supersaturating it with $BaCl_2$ solution.

The rinsed sediment was treated with a solution comprising 4N hydrochloric acid with 5% $SnCl_2$ for the dissolution of calcite. The 5% is included $SnCl_2$ to attempt to mitigate the oxidation of pyrite during acidification because pyrite grains within carbonate rocks can contaminate the CAS signal during acidification (Marenco et al., 2008). Pyrite oxidation during CAS extraction is thought to occur by reaction of pyrite with Fe-oxides, not directly with O_2. The addition of $SnCl_2$ reacts with Fe-oxides more readily than pyrite, limiting the potential impact on final $\delta^{34}S$ values. Insoluble residues were removed via vacuum filtration, thoroughly rinsed with DI water, dried and archived. The filtrate following acidification was saturated with 20% barium chloride ($BaCl_2$) solution to precipitate the dissolved sulfate, as barium sulfate ($BaSO_4$). In order to precipitate the maximum amount of sulfate, the solution was allowed to sit for at least 3 days to ensure complete precipitation. Then the barite was collected via filtration, dried, weighed and stored prior to analysis.

Pore-Water Sulfate Extraction

In order to determine the potential of overprint on CAS $\delta^{34}S$ values by pore water sulfate we analyzed the $\delta^{34}S$ values of pore-water sulfate from site U1409. Pore waters samples were extracted from squeeze cake samples taken shipboard immediately following core recovery. Samples were loaded into a piston anvil press and filtered into gas-tight syringes (Norris et al., 2014). Pore water splits were killed with saturated mercuric chloride to limit the potential of microbial activity. Pore water sulfate concentrations were determined shipboard via ion chromatography (Norris et al., 2014).

In order to obtain about 2mg of $BaSO_4$ for analyses, we used 2.5 mL of each pore-water sample, with sulfate concentrations between 20-30 mM (Norris et al., 2014). We employed extraction methods from Carmody et al., (1998) and Böttcher et al., (2004). These samples were initially filtered with a membrane filter and acidified to a pH of 4. The samples were then heated to 90ºC to drive off any dissolved CO_2. Any potential dissolved organic matter was removed with a few drops of 5% hydrogen peroxide. If the peroxide-treated solution turned yellow/brown, it was heated at 90ºC until to clarity (~30 minutes). Once the pore-water samples were heated and acidified, they were supersaturated with 10% $BaCl_2$ solution to precipitate pore-water sulfate as barium sulfate ($BaSO_4$). Precipitation was instantaneous, but samples were left for 12 hours to ensure complete precipitation. The resulting barium sulfate was filtered and dried in a drying oven overnight at 30ºC. Measurements of extracted $BaSO_4$ corresponded to initial estimates of $BaSO_4$ on the basis of sulfate concentrations, consistent with complete precipitation.

Analysis

Sulfur isotope measurements were performed on an Isoprime 100 IRMS continuous-flow stable isotope mass spectrometer coupled to an Elementar Isotope Cube elemental analyzer. Flow and combustion conditions within the elemental analyzer were as follows: He flow was 230 ml min^{-1}, the oxygen pulse was set at 90 seconds, oxidation furnace temperature was 1150ºC, the reduction furnace temperature was 880ºC, sulfur trap purge temperature was set to 230ºC to maximize peak heights for small samples and to mitigate the potential of memory effects. The collected extracted barium sulfate samples from CAS and pore-water sulfate extraction were weighed (~0.500 g) in tin cups with a tungsten oxide or vanadium pentoxide catalyst to facilitate combustion in the EA (elemental analyzer). Both accelerants proved to be equally efficient during analysis in the reproducibility of sulfate standards.

The GAPP Lab Isoprime 100 has a 7-Faraday cup collector array capable of the analysis as SO^+, as well as SO_2^+ for $\delta^{34}S$. Analysis of SO^+ allows for improved data precision and accuracy because it limits isobaric interferences between ^{34}S and ^{18}O (Baubalys et al., 2007). All data are reported on the V-CDT scale (Canyon Diable Troilite) using permil notation (see below).

$$\delta^{34}S_{sample} = \frac{\left(\frac{^{34}S}{^{32}S}\right)_{Sample} - \left(\frac{^{34}S}{^{32}S}\right)_{CDT}}{\left(\frac{^{34}S}{^{32}S}\right)_{CDT}} \times 1000.$$

We utilized the IAEA Seawater Sulfate (+20.3‰). Sample normalization was achieved using the 2-pt correction scheme described in Coplen et al. (2006). Barite extracted from sediment samples were run at least 2x and in some case 4x separately. Demonstrated analytical reproducibility on sample material was +/- 0.04 to 0.3‰.

Results

The initial CAS isotopic results were corrected to the IAEA standards, and the values for the $\delta^{34}S$ CAS of each sample is an average value from multiple runs. The error bars indicate the variation between the $\delta^{34}S$ values among multiple runs from the average values (*Figure 9 & Table 1*). The ages for the $\delta^{34}S$ values were calculated on the basis of the closest chronostratigraphic or biostratigraphic datums, according to the 2012 Geologic Time Scale (Gradstein et al., 2012; Norris et al., 2014). The error in age estimates was formulated on an average % error between different biostratigraphic datums, assigned from nannofossil and

radiolarian biozones, and chronostratigraphic datums. This averaged calculated error was applied to samples in *Figures 9-14*.

CAS $\delta^{34}S$ values range from +15‰ to +25‰. Over the duration of the 4‰ positive excursion reported in the Paytan et al. (1998) our data vary from 18 to 24‰. Despite a difference in the magnitude, this positive excursion still mirrors the timing of the marine barite curve (*Figure 1*). The $\delta^{34}S$ values are plotted by site in *Figure 9* and indicate that site U1408 is characterized by more depleted $\delta^{34}S$ values. $\delta^{34}S$ values are binned by the abundance of carbonate in each sample (*Figure 10*). The samples with higher $CaCO_3$ content more closely mirror the Paytan et al. (1998) (*Figure 11*). The Paytan et al. (1998) marine barite curve, which has been adjusted to the 2012 Geologic Timescale based off of chronostratgraphic datums (Gradstein et al., 2012) (Paytan and Gray, 2012). The comparison between the $\delta^{34}S$ record and the $\delta^{13}C$ and $\delta^{18}O$ compilation from Cramer et al. (2009) were adjusted to the 2012 Geologic Time Scale (personal communication Kristy Edgar and Pincelli Hull) (*Figures 12 and 13*).

The percentage of CAS is plotted relative to $\delta^{34}S$ values in *Figure 15*. *Figure 16* shows the relationship of %CAS in the whole samples relative to the %CAS in the carbonate content of each sample, and *Figure 17* shows the variation in $\delta^{34}S$ values relative to the marine barite curve in comparison to %CAS. In *Figure 18* the changes in pore-water sulfate $\delta^{34}S$ composition and concentration vary with depth and are superimposed with $\delta^{34}S$ CAS values to determine the likelihood of CAS contamination by interstitial pore-waters. The pore-water sulfate plots show enrichment in sulfate $\delta^{34}S$ values but depletion in the sulfate concentrations with depth.

Discussion

The Cenozoic sulfur isotope study of Paytan et al. (1998) was a landmark work that illustrated the plasticity of the sulfur cycle by documenting large changes in the sulfur isotope composition of seawater sulfate. The prior understanding was that sulfate concentrations were relatively constant during the Phanerozoic because sulfate values should correspond with atmospheric oxygen levels, which have remained relatively stable for the past 500 Ma. Since this time, several authors have attempted to understand the nature of sulfur cycle variability in the Cenozoic, most notably the work of Kurtz et al (2003) and Wortmann and Paytan (2012). These two works focused on the Early Eocene sulfur cycle and suggest two mechanisms, anoxia vs. evaporite weathering, to explain the cause of this $\delta^{34}S$ increase ~50 Ma.

Early Eocene Sulfur Cycle

Seawater Sulfate Concentrations were low in the Cretaceous

The late Cretaceous seawater sulfate reservoir was much smaller than the modern, and the sulfate reservoir remained smaller through the onset of the Paleocene (Horita et al., 2002, Timofee et al., 2006). A smaller sulfate reservoir during the Paleocene might suggest that the sulfate reservoir was more sensitive to sulfate inputs/outputs during the early Eocene. Turchyn and Shrag (2004) found significant variation in the oxygen isotopic values of seawater sulfate ($\delta^{18}O_{SO4}$) during the Cenozoic. They attribute to changes in the sulfate flux from increased/decreased evaporate and pyrite weathering. Despite these changes, the isotopic composition of sulfur from seawater sulfate remained relatively static from the middle Eocene to today (Paytan et al., 1998).

Eocene Climatic Changes

Better constraints on the response of the sulfur cycle during periods of dramatic climate change can illuminate changes in the major geochemical systems, including the cycling of carbon. The Eocene is one of the warmest intervals of geologic time for which there exists a fairly complete geologic record. This interval of warmth is frequently used as an analog for understanding the effects of anthropogenic induced climate change (Cui et al, 2011). Better constraints on the response of the sulfur cycle during periods of dramatic climate change can illuminate changes in the major geochemical systems, including the cycling of carbon. The early-to-middle Eocene is characterized by several negative $\delta^{13}C$ excursions within planktonic and benthic foraminifera stable isotope records. Gray, clay-rich layers are common in early Eocene sequences, which indicates the dissolution of calcium carbonate under a relatively shallow carbonate compensation depth (Sexton et al., 2011). Better constraints on the timing and duration of the positive $\delta^{34}S$ excursion during the early-middle Eocene can provide more clarity on the response of the sulfur cycle to warming (Zachos et al., 2005; 2008; Sexton et al., 2011) and influences of warmth on ocean circulation (Kaiho, 1991) through the PETM and Early Eocene Climatic Optimum (EECO).

"Localized Anoxia Hypothesis"

Kurtz et al., (2003) proposed that widespread euxinic conditions were pervasive during the early Eocene (~50 Ma) on the basis of box model calculations of organic carbon and pyrite burial. This putative increase in anoxic and sulfidic water masses would have led to a compensatory increase in pyrite burial resulting in elevated $\delta^{34}S$ sulfate values. Long-term warmth following the PETM (Paleocene-Eocene Thermal Maximum) through the EECO may have contributed to ocean stratification and more sluggish ocean circulation during the early

Eocene (Kurtz et al., 2003; Kaiho, 1991). These conditions may have been advantageous for an increase in anaerobic respiration in the deep sea, likely increasing rates of MSR (microbial sulfate reduction) and pyrite burial fluxes. Early Eocene sea level rise (Miller et al., 1997) may have flooded continental shelves, and enhanced MSR in more enclosed continental basins (Kurtz et al., 2003). Although Kurtz et al., (2003) attribute this spike in pyrite burial to widespread euxinic conditions, our samples do not suggest any geochemical evidence of euxinic or anoxic conditions, but coastal regions of the Northern Tethys and the Arctic basin exhibit euxinic/anoxic deposits (Dickson et al., 2014; Stein et al., 2006). Assuming that pyrite burial from amplified MSR in anoxic pockets of the ocean was strong enough, could localized anoxia influence global seawater sulfate $\delta^{34}S$ values? The Tethys Ocean became increasingly enclosed during the late Cretaceous, so it may have been more susceptible to stratification and estuarine circulation through the early Cenozoic. Although the Tethys was still well connected to Indian Ocean and sea level was high during the Early Eocene (Miller et al., 1997), the Eocene outcrops along the Northern edges of the former Tethys Ocean exhibit geochemical evidence of anoxia (Dickson et al., 2014). These anoxic deposits are attributed to an increase in primary productivity from phosphorous recycling under euxinic conditions (Adams et al., 2010). Dickson et al., (2014) ascribe this increase in nutrient availability to enhanced rates of continental weathering during the PETM from increased precipitation in the sub-tropics (Schmitz and Pujalte, 2007).

The PETM also marked a shift in the oxygenation of the Arctic Ocean. Cores from IODP EXP 302 indicate a shift from oxic to euxinic conditions following the PETM (Stein et al., 2006), and some Eocene marine sedimentary sections that border the Arctic Ocean also display indications of euxinia (Cui et al., 2011). Pyrite burial increased in the Early Eocene, and C/S ratios suggest that the Arctic Ocean remained euxinic through the middle Eocene (Stein et al.,

2006). Stein et al., (2006) attribute Arctic euxinic conditions to density stratification caused by an increased input of freshwater from an amplified hydrologic cycle in the Arctic during the PETM (Pagani et al., 2006). A high abundance of the aquatic fern, Azolla, in IODP EXP 302 cores suggests that the Arctic Ocean had relatively fresh surface waters because Azolla cannot tolerate high salinities (Brinkhuis et al., 2006). The rise of the Azolla population in the oceans does correlate with the cooling trend that follows the EECO (Early Eocene Climatic Optimum) around 50 Ma and the drawdown of atmospheric CO_2 (Brinkhuis et al., 2006; Beerling and Royer, 2011) (*Figure 14*).

The warmer Eocene climate could have reasonably lead to the stratification of the ocean and enhanced localized anoxia/euxinia in areas of high freshwater flux. An increase in the burial of organic carbon corresponding to anoxic conditions could possibly cause a complimentary spike in pyrite burial. The additional problem that this hypothesis faces is why the $\delta^{34}S$ record remains ^{34}S-enriched and stable through the remainder of the Cenozoic. An interval of enhanced pyrite burial could cause enrichment in the $\delta^{34}S$ values at the expense of the sulfate reservoir. However, this would ultimately result in less stability in the $\delta^{34}S$ record of seawater sulfate. Amplified pyrite burial alone is an improbable mechanism to cause this middle Eocene positive excursion in the $\delta^{34}S$ values of seawater sulfate because pyrite burial is inconsistent with the growth of the seawater sulfate reservoir during the early Eocene.

This balance of data suggest that the seawater sulfate reservoir was smaller during the onset of the Eocene and into the Paleocene (Horita et al., 2002; Lowenstein et al., 2003). Estimates of seawater sulfate concentrations from fluid inclusion data (Horita et al., 2002) and estimations of ocean water volumes (Hay et al., 2006), early Paleocene seawater had a marine sulfate budget (1.898×10^{21} g sulfate) less than half of modern seawater (3.840×10^{21} g sulfate).

Paleocene seawater was ~0.013% sulfate, mid-Eocene seawater was ~0.018% sulfate, and modern oceans are ~0.028% sulfate. The mid-Eocene marine sulfate budget was still lower than the modern (2.576×10^{21} g sulfate) but still exhibited a significant increase from the Paleocene. The dramatic increase in the marine sulfate budget (6.78×10^{20} g sulfate over ~12 Ma) from the Late Paleocene to the Early Eocene outpaces the modern estimations of net inputs of sulfate (Bottrell and Newton, 2006; Walker, 1986).

"Evaporite Weathering Hypothesis"

The Eurasia-India collision and subsequent uplift of the Himalayans initiated ~50 Ma (Patriat and Acheche, 1984), but the exact temporal resolution of this tectonic event still remains hotly debated and has yet to be better constrained. This Himalayan uplift provides a mechanism for increased availability of weatherable material as continental margins laden with evaporite deposits were uplifted and eroded (Wortmann and Paytan, 2012; Raymo and Ruddiman, 1992). A negative excursion in seawater sulfate $\delta^{34}S$, from +20‰ to +15‰ around 120 Ma, is attributed to the opening of the South Atlantic Ocean and massive evaporite deposition, which decreased seawater sulfate concentrations (Wortmann et al., 2007; Burke and Sengor, 1988). Reduced concentrations of sulfate in the global ocean acted to decrease MSR rates and pyrite burial, thereby resulting in the ^{34}S-depletion in the seawater sulfate reservoir.

Although any evidence for extensive evaporite deposition on the Himalayans has long since been eroded away, quantitative reconstructions of seawater salinity through the Phanerozoic suggest that a significant amount of halite deposition occurred during the Late Cretaceous (Hay et al., 2006) and may have been available for weathering during the onset of the Himalayan uplift. The addition of sulfate via weathering may have initially decreased the $\delta^{34}S$ of

seawater because evaporites have slightly depleted $\delta^{34}S$ values relative to seawater $\delta^{34}S$. Higher sulfate concentrations will ultimately result in an increase of seawater $\delta^{34}S$ values through the stimulation of MSR and the subsequent increase in pyrite burial.

An additional source of weathering-derived sulfate may also have been derived from the closure and uplift of the Western Interior Seaway associated with the Laramide Orogeny. Higgins and Schrag, (2006) implicate oxidation of organic carbon from rocks and the sediment of the Western Interior Seaway as a contributing factor in the carbon pulse at the PETM (Paleocene Eocene Thermal Maximum). Increased inputs of organic carbon may have contributed to enhanced MSR rates because the availability of organic material is more pertinent for MSR than sulfate availability (Kao et al., 2004).

Eurasia-India Collision

Paleomagnetic data largely confirm that the initial collision between India and Eurasia began ~50 Ma (Patriat and Achache, 1984), but whether that initial collision lead to instantaneous uplift is still debated. Molnar and Tapponnier (1975) argue that large-scale vertical motion of the Himalayas did not occur until the Oligocene, and Harrison et al., (1992) argue that uplift was stalled until the early Miocene. Seawater Sr isotope ratios, which are utilized as a proxy for continental weathering, remain relatively flat between 40-60 Ma (Richter et al., 1992). Even though evaporite weathering does not influence the seawater Sr record, the increase in Sr isotope ratio values associated with Himalayan uplift does not occur until well past 40 Ma (Richter et al., 1992). Additionally, the late Cretaceous had low seawater sulfate concentrations, so many Cretaceous brines/evaporate sequences had relatively low concentrations of sulfate (Timofee et al., 2006). Cretaceous evaporite sequences are still widespread and these sequences

that are present in the northern coast of Brazil, the Republic of Congo, and Thailand have very low concentrations of sulfate (Wu et al. 1990; Timofee at al., 2006). If the evaporite deposits eroded from the Himalayas were precipitated during the Late Cretaceous, they would have had low sulfate concentrations and been a minor contributor to the early Eocene sulfate reservoir. In order for the uplift of the Himalayas and subsequent massive evaporite dissolution to be the mechanism for this positive $\delta^{34}S$ excursion, the timing of the uplift should occur before 50 Ma and the eroded evaporite deposits should have had higher sulfate concentrations, possibly originated from older, more sulfate-rich sequences.

"Volcanic Triggering Hypothesis"

Volcanic activity may have also influenced Paleogene seawater chemistry and contributed to the variability in the sulfate reservoir via the addition of volcanic sulfur (e.g. Adams et al., 2010). High levels of volcanism and hydrothermal activity characterized the late Cretaceous (Adams et al., 2010; Self et al., 2008; Timofee et al., 2006). Flood basalts in Greenland and Denmark were erupting during the early Eocene (Storey et al., 2007). Although volcanic-derived sulfur is ^{34}S-depleted relative to seawater sulfate (0-3.5 ‰), the addition of volcanic sulfur can easily increase the size of the sulfate reservoir (Arthur, 2000). The decrease in $\delta^{34}S$ in the late Paleocene, prior to this contentious positive excursion at 50 Ma, may be related to volcanic inputs of ^{34}S-depleted, volcanic sulfur (Arthur, 2000).

The mid-Cretaceous is characterized by increased ocean-crust production rates and increased volcanism that has been attributed to a superplume at the core-mantle boundary, which coincides with a prolonged period lacking magnetic reversal (Larson, 1991). Cretaceous seawater chemistry from halite inclusions suggests that the Cretaceous had amplified

hydrothermal activity (Timofee et al., 2006; Lowenstein et al., 2001). The Deccan Traps in India was a massive volcanic event that occurred between 67-65 Ma (Self et al., 2008). Glass compositions from the Deccan flood basalts indicate that the magmatic melt of origin had very high sulfur concentrations and released massive amount of SO_2 into the atmosphere (Self et al., 2008). Self et al., (2008) calculated that the annual SO_2 release from the Deccan traps would have been several orders of magnitude greater than anthropogenic emissions of SO_2. This excess of atmospheric SO_2 would have eventually increased seawater sulfate concentrations and possibly amplified erosional rates from acid rain over the duration of eruption. The Sr isotope ratios of seawater increase ~65 Ma, corresponding to an increase in continental weathering (Richter et al., 1992), and the Paytan et al. (2008) marine barite curve exhibits a 2‰ $\delta^{34}S$ depletion ~65 Ma, possibly linked to an increase in ^{34}S-depleted sulfate. Widespread volcanism during the late Cretaceous could be a possible mechanism for increasing the size of the marine sulfate reservoir during the early Eocene. According to $^{40}Ar/^{39}Ar$ age dates, Greenland and Northern Europe had a breakup about ~61 Ma (Storey et al., 2007). This rift lead to amplified volcanic activity in Greenland and Denmark ~55 Ma, during the PETM. Contact metamorphism of carbonate-rich sediments or sulfide-rich sediments could release massive amounts of CO_2 and SO_2 (Ganino and Arndt, 2009).

A Likely Mechanism for this Excursion?

Our data do not provide a clear-cut understanding of this excursion nor a mechanism (*Figure 13 &14*). Since the timing of the $\delta^{34}S$ excursion aligns at 50 Ma, it is unlikely that the mechanism for this excursion could be only evaporite weathering from the Himalayan uplift over such a short period of time. The massive dissolution of evaporite deposits would have initially decreased the $\delta^{34}S$ value of seawater before amplified MSR drove $\delta^{34}S$ enrichment. In order for

this mechanism to work, Himalayan uplift and evaporate dissolution would need to occur between 60-50 Ma, which is much earlier than most estimates of uplift (Molnar and Tapponnier, 1975). Fluid inclusion data (Horita et al., 2002) indicate that seawater sulfate concentrations dramatically increased from the Late Creataceous to the middle Eocene. Amplified pyrite burial is a sink for seawater sulfate, so localized anoxia/euxinia cannot be the primary mechanism for this excursion. Increased volcanism during the late Creataceous and during the PETM would add sulfate to the marine reservoir as well as carbon and amplify pyrite burial, thus it is the most likely of the three mechanisms to be the cause of this $\delta^{34}S$ excursion.

Variability in the CAS Data

Several previous studies (Ohkouchi et al., 1999; Turchyn et al., 2009) have found that the CAS signal can be quite variable across the same stratigraphic unit or within carbonates that do exhibit clear indications of alteration. Since CAS content is associated with the amount of carbonate within a given sample, CAS values were binned according to wt. % $CaCO_3$ (*Figures 10 & 11*). Samples with lesser amounts of calcium carbonate exhibit more deviation from the marine barite record than CAS samples with higher calcium carbonate contents. The anomalously enriched CAS $\delta^{34}S$ values, as well as depleted values, are associated with low amounts of CAS within the sample (*Figure 15 & Figure 17*). The amount of CAS in a sample (or %CAS) was calculated from the mass of the whole sample and the calcium carbonate content. There should be a positive correlation between the amount of CAS in a sample and the amount of CAS in the carbonate, which indicates that the only source of sulfate in these samples is CAS-derived. The few samples that do not follow this linear trend are assumed to have additional sources of non-CAS sulfur, most likely oxidized pyrite.

Since the most variable CAS $\delta^{34}S$ values are associated with lower %CAS concentrations, samples with lower amounts of CAS may be more sensitive to pyrite oxidation or pore-water contamination. Diagenesis or recrystallization may cause a loss of CAS and the incorporation of non-primary CAS into the carbonate structure. Samples from ODP EXP 207 displayed significant overgrowth on forams and relatively poor carbonate preservation despite the high carbonate content. They also had had low %CAS concentrations and enriched $\delta^{34}S$ values. If CAS concentration is a possible constraint on CAS variability, then could fluctuations in the sulfate concentrations of seawater influence the viability of CAS data? Studies on the influence of meteoric diagenesis on CAS indicate that meteoric diagenenesis usually causes a decrease in CAS concentration because meteoric waters are usually depleted in sulfate relative to seawater (Gill et al., 2008). These studies also found that aragonite and calcite incorporate CAS in different concentrations (Gill et al., 2008). Aragonite incorporates on average significantly higher concentrations of CAS than calcite. Since the sulfate anion is larger than the carbonate anion, perhaps aragonite, which has a higher abundance of the smaller magnesium cations relative to the larger calcium cations, can incorporate more CAS into the calcium carbonate structure. This positive excursion does correspond roughly to the transition from calcite to aragonite seas.

Pore-Water Sulfate Data

To better constrain possible diagenetic influences on CAS values, we utilized complimentary pore-water sulfate data. The $\delta^{34}S$ pore-water sulfates values from site U1409 become increasingly ^{34}S-enriched with depth as the concentration of the pore-water sulfate decreases. The relatively linear decrease in sulfate concentration above 140 mbsf is consistent with diffusion of sulfate from seawater. The inflection in $\delta^{34}S$ values and sulfate concentrations

at 140 mbsf is likely the result of localized sulfate reduction at depth below a chert layer, which acts like an aquiclude by holding water (*Figure 18*). The overall decrease in sulfate concentrations with depth is likely related to consumption of sulfate by MSR in organic matter-rich black shales that underlie the South East Newfoundland Ridge sites (Norris et al., 2014). Rennis and Turchyn (2014) found that CAS is sensitive to overprinting from pore-water sulfate when sedimentation rates and MSR rates are elevated. In this study we found that the pore-water $\delta^{34}S$ values are generally higher than the CAS $\delta^{34}S$ values. Since the pore-water $\delta^{34}S$ values show no clear relationship with the $\delta^{34}S$ of CAS, pore-water contamination is not a likely source for enriched $\delta^{34}S$ CAS values.

The Problem of Pyrite Oxidation

Marenco et al. (2008) and Mazumdar et al. (2008) discovered that pyrite oxidation by metal oxides can contaminate the CAS signal. In order to mitigate accidental pyrite oxidation, we utilized 5% $SnCl_2$ in our HCl solution as suggested by the Lyons group at UC Riverside, but pyrite oxidation clearly still occurred in a several samples (*Figure 16*). All of the anomalously depleted $\delta^{34}S$ CAS values are from site U1408 (*Figure 9*). The samples from site U1408 were very clay-rich and had sulfide mottling between 42.3-70.86 mbsf (Norris et al. 2014). Despite utilizing $SnCl_2$ during acidification (unlike Marenco et al., (2008) studies), the high clay content of these samples may have interfered with our efforts to reduce pyrite oxidation by trapping non-CAS sulfur or pyrite.

Implications for Future CAS Studies

Future CAS studies utilizing bulk carbonates could be better executed by separating the clay fraction from the coarse fraction in order to prevent secondary sulfates/sulfides from

contaminating the CAS values. Centrifuging the acidified solution may help remove oxidized pyrite. Additionally, to better constrain the sources of variability in the CAS record, future studies would benefit from complimentary CAS $\delta^{18}O_{SO4}$ records of sulfate oxygen. Variations in $\delta^{18}O_{SO4}$ CAS can indicate different inputs weathering-derived sulfate (Turchyn and Shrag, 2004), and $\delta^{18}O_{SO4}$ data can indicate pyrite oxidation if the $\delta^{18}O_{SO4}$ values match the lab water $\delta^{18}O$ values instead of seawater $\delta^{18}O$ (Rennie and Turchyn, 2014).

This study found that CAS concentration is closely linked to CAS $\delta^{34}S$ variability. Future studies should also target samples that have high concentrations of calcium carbonate. CAS values should be interpreted in terms of systematic changes in seawater chemistry, such as calcite/aragonite seas (Hardie, 1996; Tomofeef et al., 2006) and fluctuations in the size of the marine sulfate reservoir. More studies that focus on better constraining the incorporation of CAS into the carbonate structure are necessary to better establish the CAS proxy.

Conclusions

Our CAS record from IODP EXP 342, for the most part, mirrors the timing and magnitude of the Paytan et al. (1998) marine barite record, but the CAS record shows a great deal more variability and a larger magnitude excursion. The most dramatic shift in $\delta^{34}S$ values occurs ~50 Ma. The stability of the $\delta^{34}S$ record for the remainder of the Cenozoic suggests that there was an increase in the sulfate reservoir during the early Eocene, and seawater sulfate concentrations remained relatively high into the modern. Although the data from this study do not provide a clear mechanism for this excursion, they do provide more insight into competing theories in the literature, the Kurtz et al. (2003) "localized anoxia" hypothesis and the Wortmann and Paytan (2012) "Evaporite Weathering" hypothesis. The "localized anoxia" hypothesis is

likely a minor player because it does not lead to an increase in sulfate concentrations, but rather a decrease sulfate concentrations. The "Evaporite Weathering" hypothesis may not fit with timing of our excursion because Himalayan uplift likely occurred after our excursion. This study proposes that an increase in volcanically derived sulfur into the marine reservoir during the late Cretaceous and early Eocene may have lead to an increase in the size of the marine sulfate reservoir and enhanced rates of MSR, leading to this positive excursion around 50 Ma.

Samples with lower CAS concentrations tend to contribute to the variability in the CAS record by having more enriched or depleted values in comparison to the Paytan et al (1998) marine barite record. Accidental pyrite oxidation during CAS extraction, especially with clay-rich samples, contaminated several CAS samples. Higher abundances of clay may have also made it difficult to remove non-CAS sulfur during rinsing steps. The anomalously high $\delta^{34}S$ values are still not well understood. To evaluate the possible role of pore water processes we analyzed corresponding pore-waters for sulfate $\delta^{34}S$. The pore-water sulfate $\delta^{34}S$ data do not suggest a relationship with the anomalously enriched $\delta^{34}S$ CAS values. The reason for this enrichment is still not well understood, and future studies should focus on better understanding the cause of variability of CAS in this and other records.

Illustrative Figures

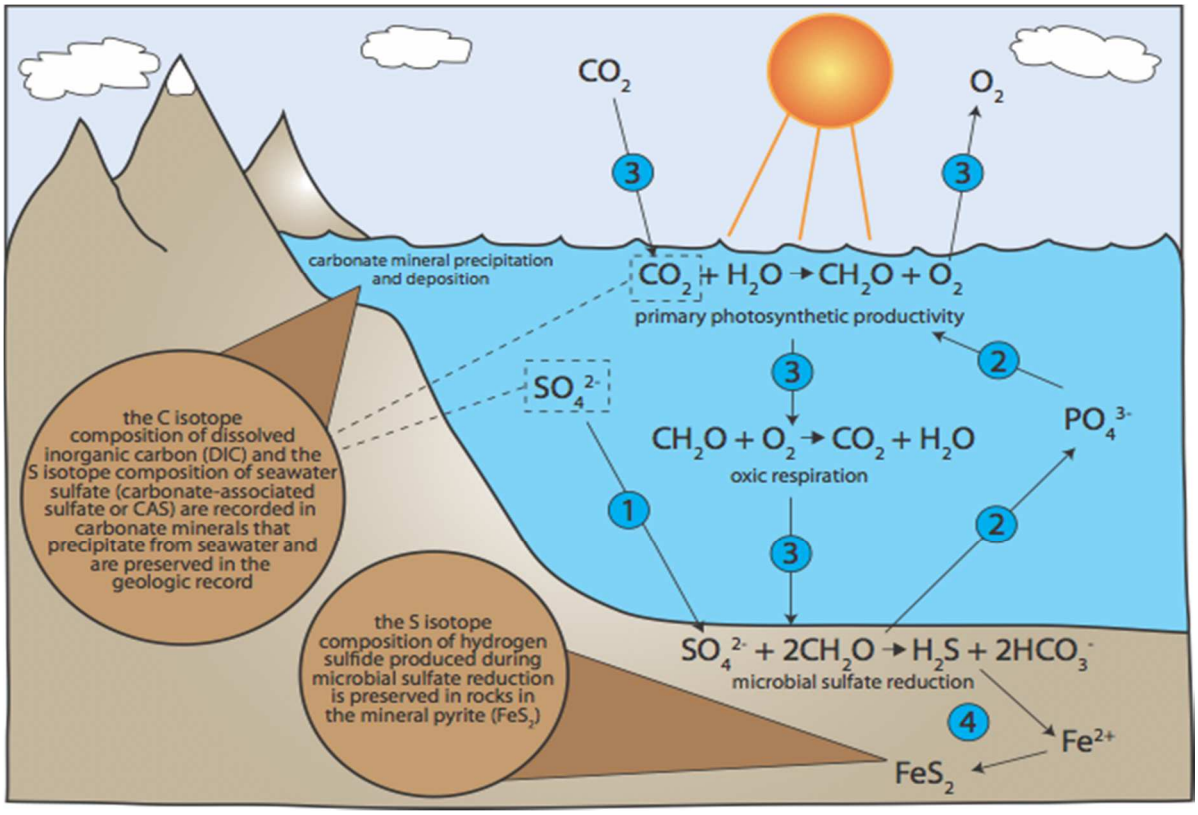

Figure 1: A rough schematic of the marine sulfur cycle: *from Matthew Hurtgen's research website, which shows the chemical reactions involved in MSR (Microbial Sulfate Reduction) in the marine sulfate reservoir.*

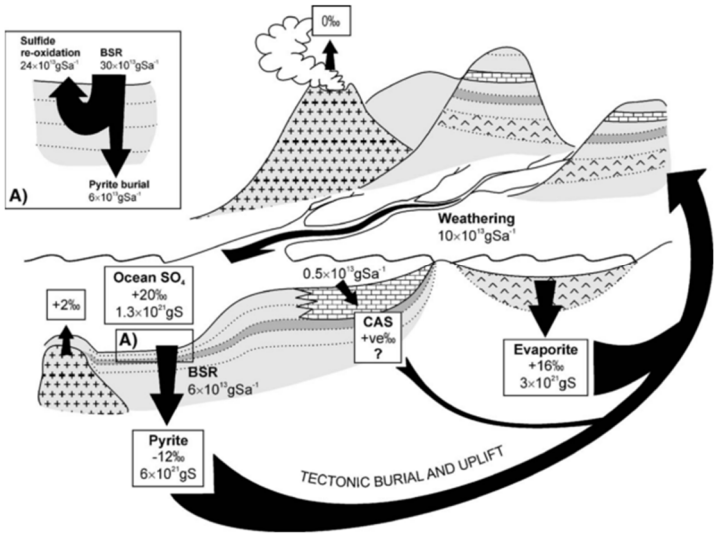

Figure 2: The major sources, sinks, and rates of burial of sulfur: *from (Bottrell and Newton, 2006) and (Walker, 1986).*

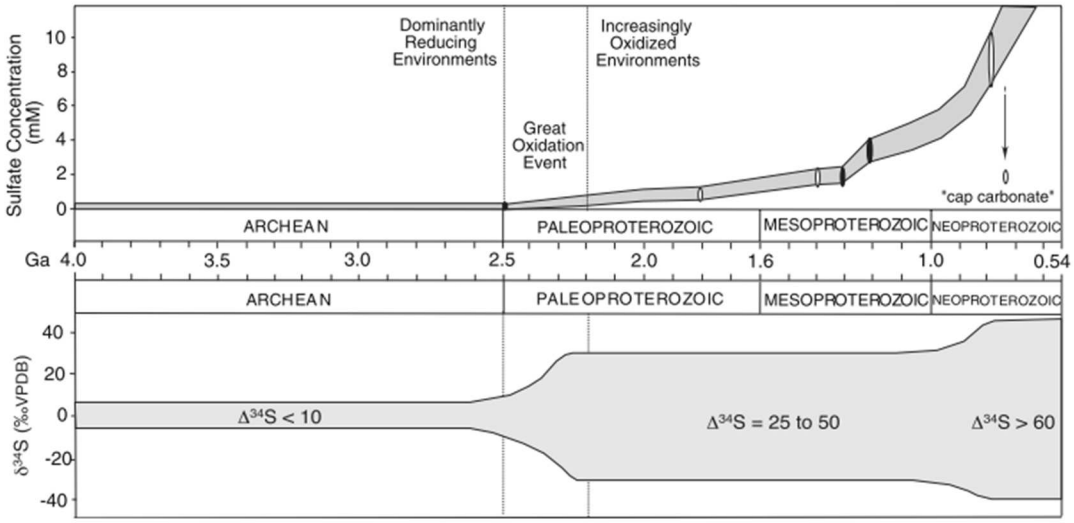

Figure 3: The Sulfate Reservoir Through Time: *This figure published by Lyons et al., 2006, used data from (Kah et al., 2004) (Habitcht et al., 2002) to show the variation in sulfur isotopic composition between the pyrite and sulfate reservoirs through Geologic time. The fractionation between the two reservoirs increases as the sulfate reservoir increases and is assumed to be relatively stable over the last 500 million years.*

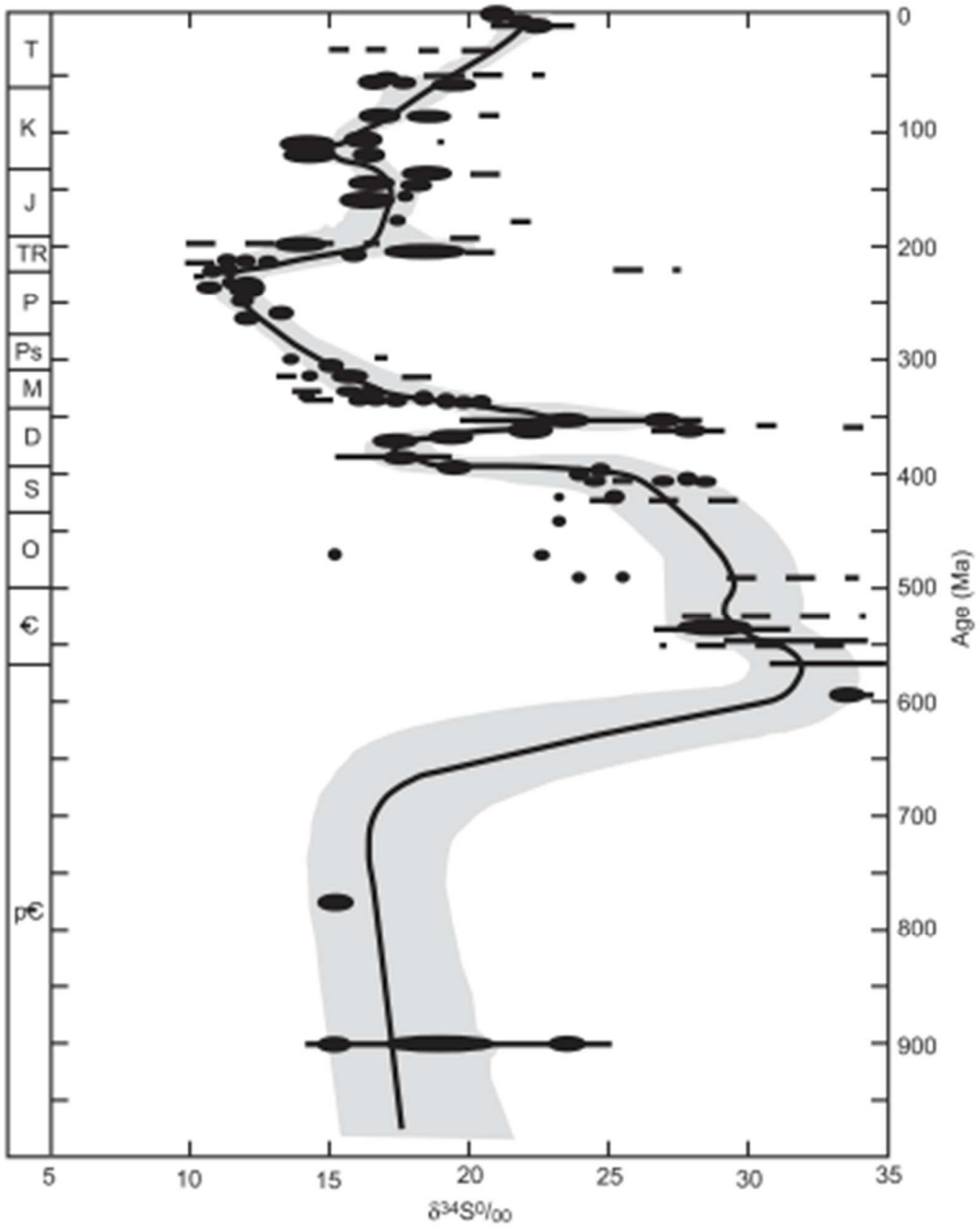

Figure 4: The "Claypool Curve": *was the first published Paleozoic and Phanerozoic $\delta^{34}S$ record of seawater sulfate from marine evaporite deposits (Claypool et al., 1980). These δ^{34} values are reported relative to the Canyon Diablo Troilite standard. This record shows the plasticity of the marine sulfate conditions during the Phanerozoic.*

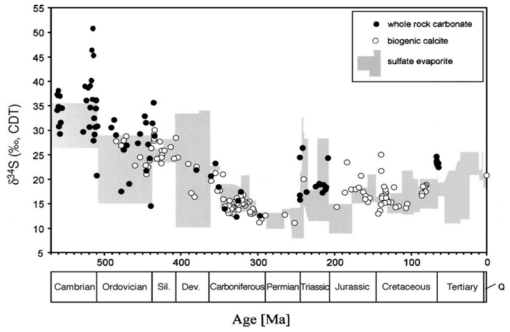

Figure 5: Phanerozoic isotopic record of seawater sulfate: $\delta^{34}S$ values from (CAS) *Carbonate-Associated Sulfates or (SSS) structurally substituted sulfates in carbonates. CAS or SSS should reflect the sulfate composition of the overlying seawater during carbonate formation (Kampschulte and Strauss, 2004) and evaporite deposits (Strauss, 1997). These δ^{34} values are reported relative to the Canyon Diablo Troilite standard. Despite relatively stable levels of atmospheric oxygen during the Phanerozoic, the $\delta^{34}S$ values are variable, even into the Cenozoic/Tertiary.*

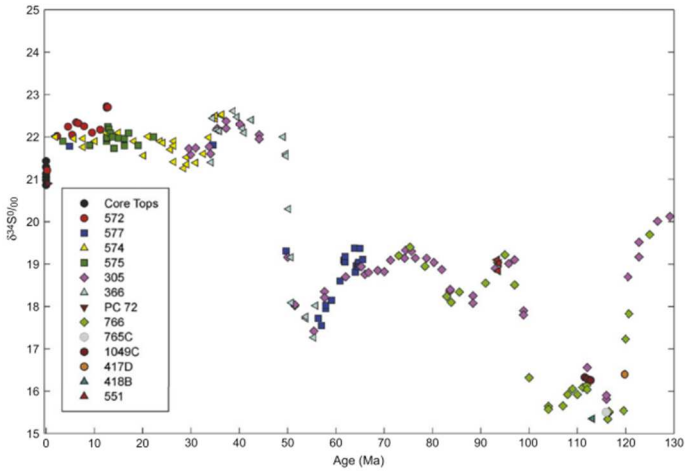

Figure 6: The "Paytan Curve": isotopic record of seawater sulfate δ34S values from authigenic marine barite from Paytan et al.(1998). *These marine barite samples are reported relative to the Canyon Diablo Troilite standard, and these samples were collected and extracted from various localities in the Pacific, Atlantic, and Indian Oceans.*

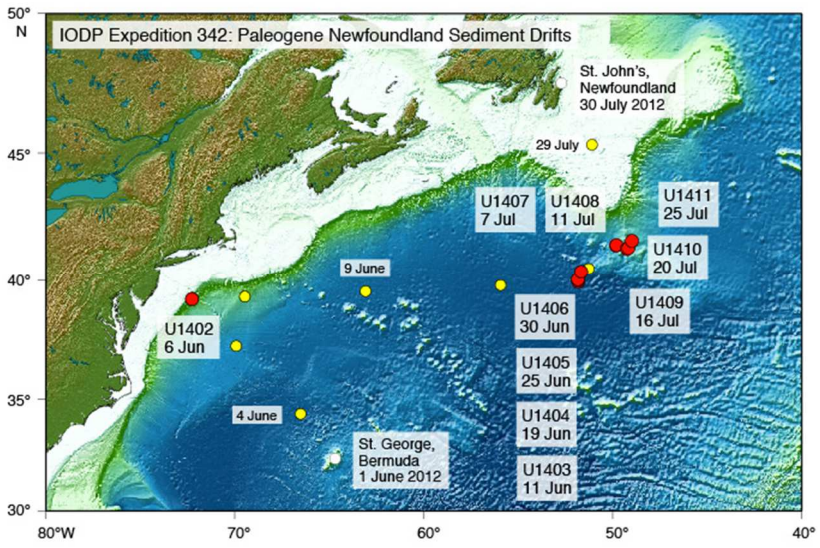

Figure 7: location of IODP sites*: where cores were extracted during IODP Expedition 342 to the Newfoundland Drifts during June and July of 2012 in the North Atlantic (Norris et al., 2014). This study uses squeeze cake samples from sites U1407, U1408, U1409, and U1410.*

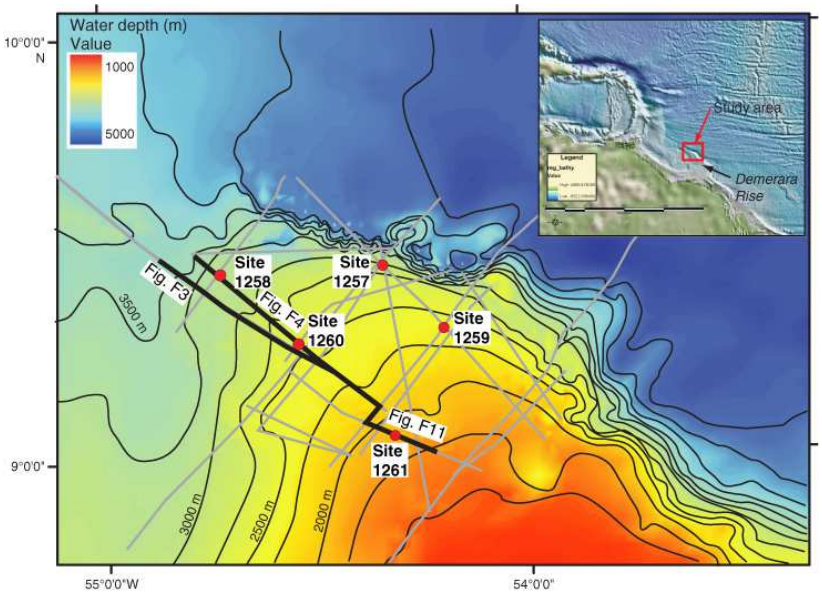

Figure 8: Locations of ODP sites*: where cores where extracted during ODP Expedition 207 to the Demerara Rise during May of 2004 in the equatorial Atlantic, off the coast of Northern South America (Erbacher et al., 2004). This study utilizes cores from sites 1258, 1260, 1261, and 1257.*

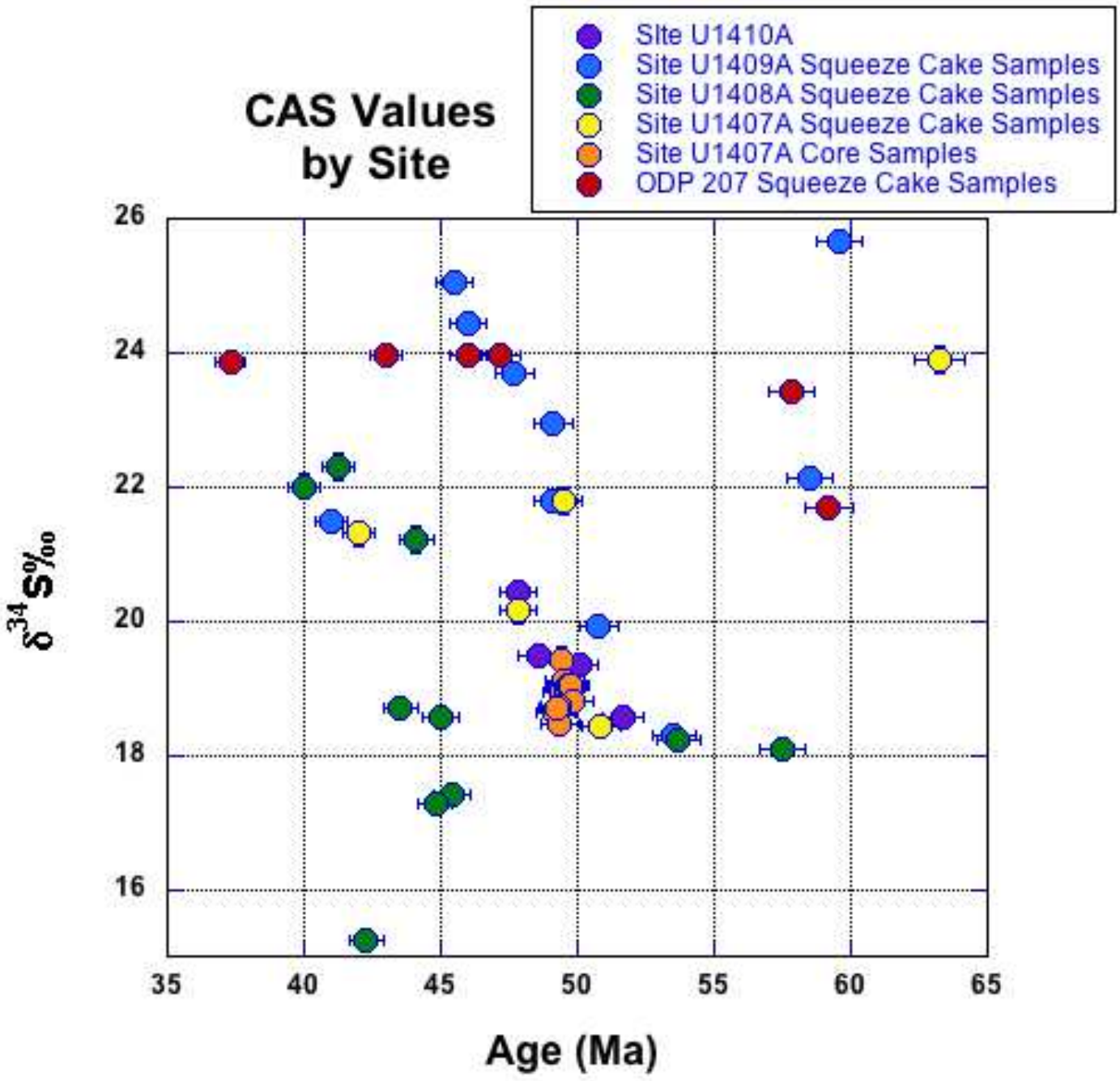

Figure 9: Bulk carbonate CAS $\delta^{34}S$ results by site: *from IODP and ODP samples are indicated by the circles, and different colors correspond to different sites. The error bars for the $\delta^{34}S$ values represent the average maximum error possible based on the variation in the $\delta^{34}S$ values (relative to the Canyon Diablo Troilite standard), but the error bars are less than the size of the circles. The error in the age estimations from biostratigraphic and chronostratigraphic datums is from Norris et al (2014).*

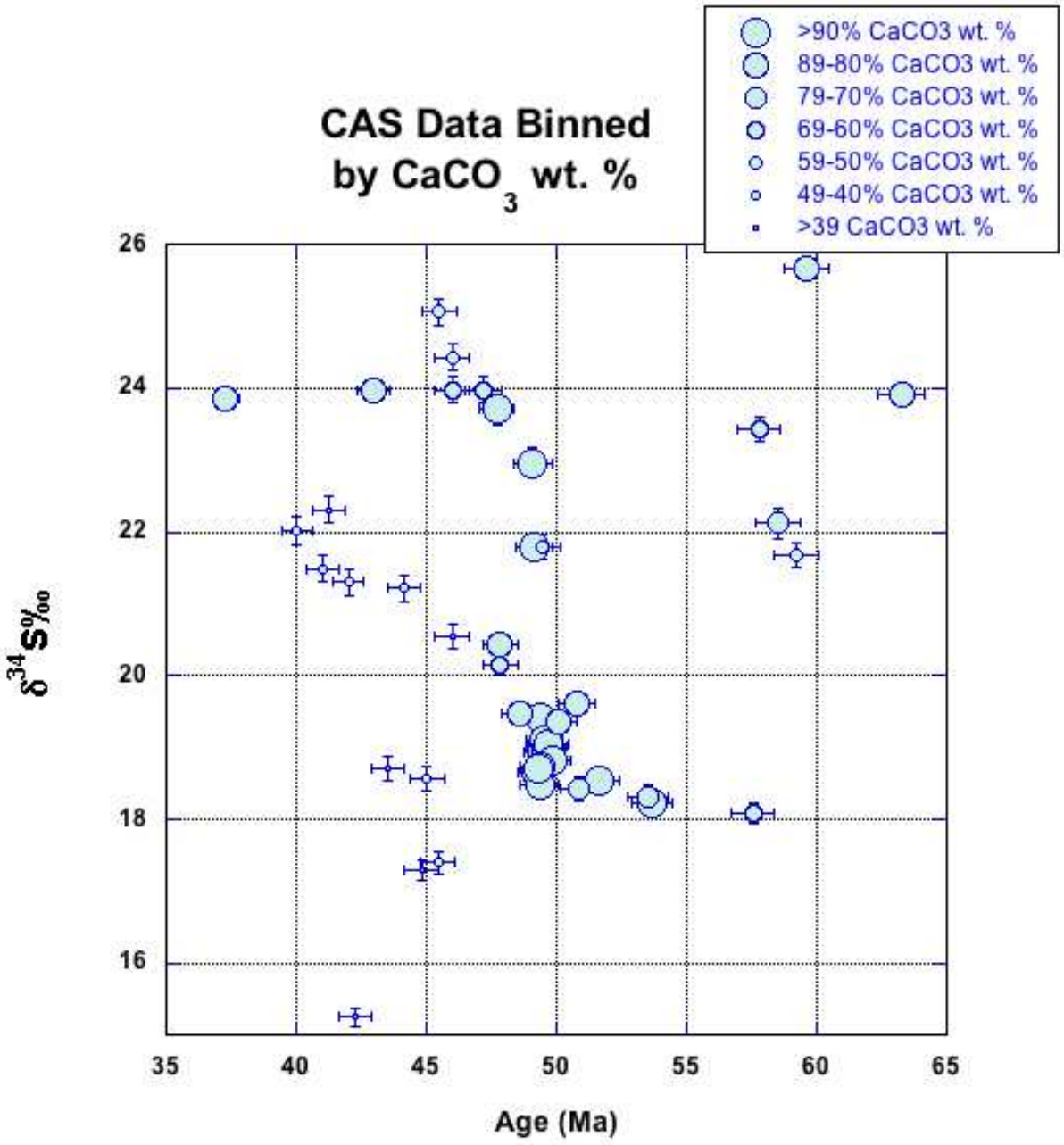

Figure 10: The CAS $\delta^{34}S$ results binned by CaCO3 wt. %: *The larger sized circles correspond to samples that have a higher concentration of $CaCO_3$. The error bars for the $\delta^{34}S$ values represent the average maximum error possible based on the variation in the $\delta^{34}S$ values (relative to the Canyon Diablo Troilite standard). The error in the age estimations is averaged from differences in biostratigraphic and chronostratigraphic datums is from Norris et al (2014).*

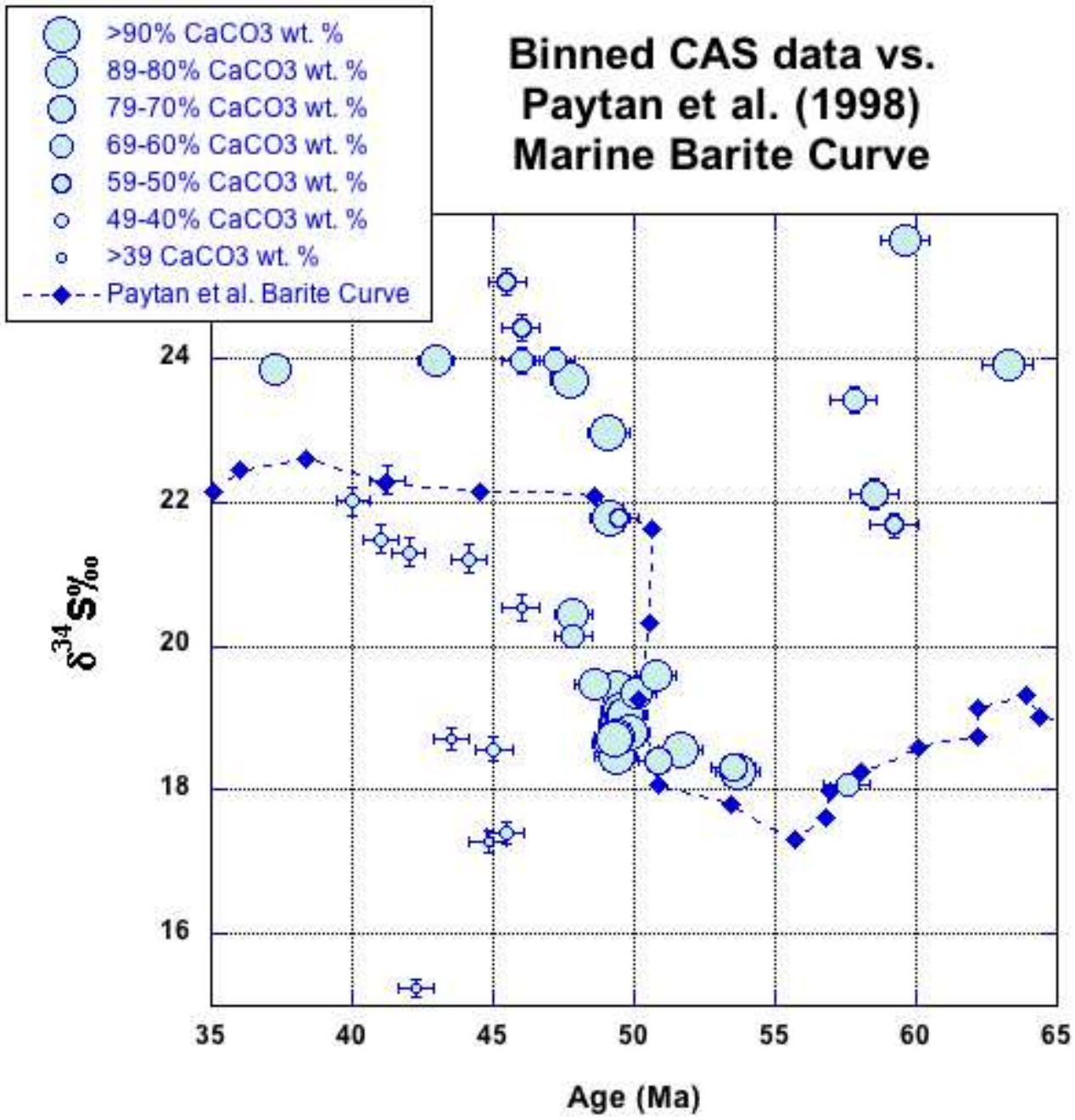

Figure 11: The binned CAS $\delta^{34}S$ results and plotted in comparison to the Paytan et al. (1998): *Bulk carbonate CAS $\delta^{34}S$ results from IODP and ODP samples are binned according to $CaCO_3$ wt. % and plotted in comparison to the Paytan et al. (1998) marine barite curve. Our CAS record shows more variability than the marine barite curve.*

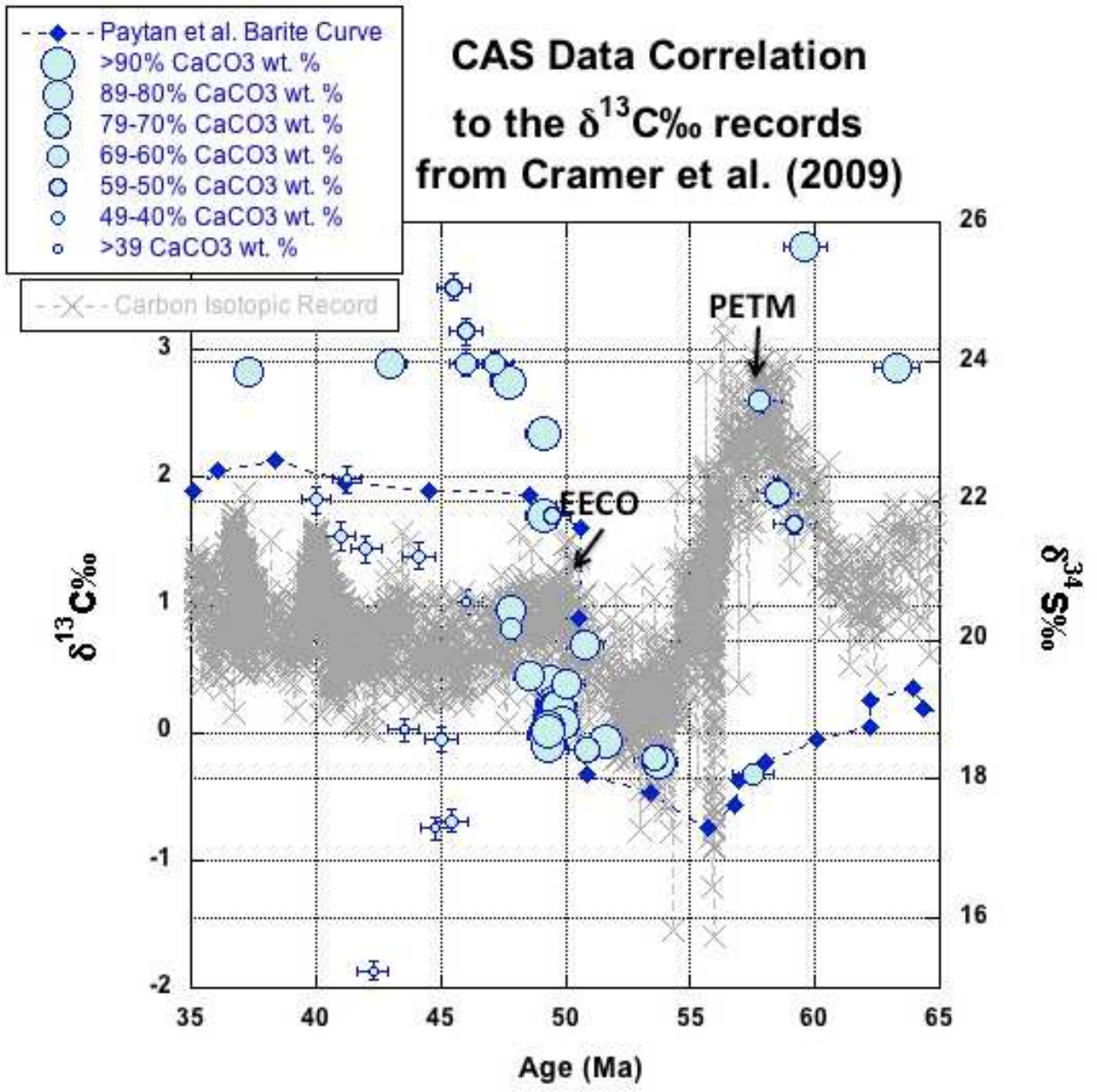

Figure 12: Binned CAS data with the δ^{13}C curve: *The bulk carbonate CAS δ^{34}S results from IODP and ODP samples are binned according to $CaCO_3$ wt. % and plotted in comparison to the Paytan et al. (1998) marine barite curve and the δ^{13}C curve compilation from Cramer et al. (2009) benthic foraminifera and adjusted to the 2012 Geologic Time Scale by Kristy Edgar and Pincelli Hull. There is little correlation between the δ^{13}C curve and our CAS curve.*

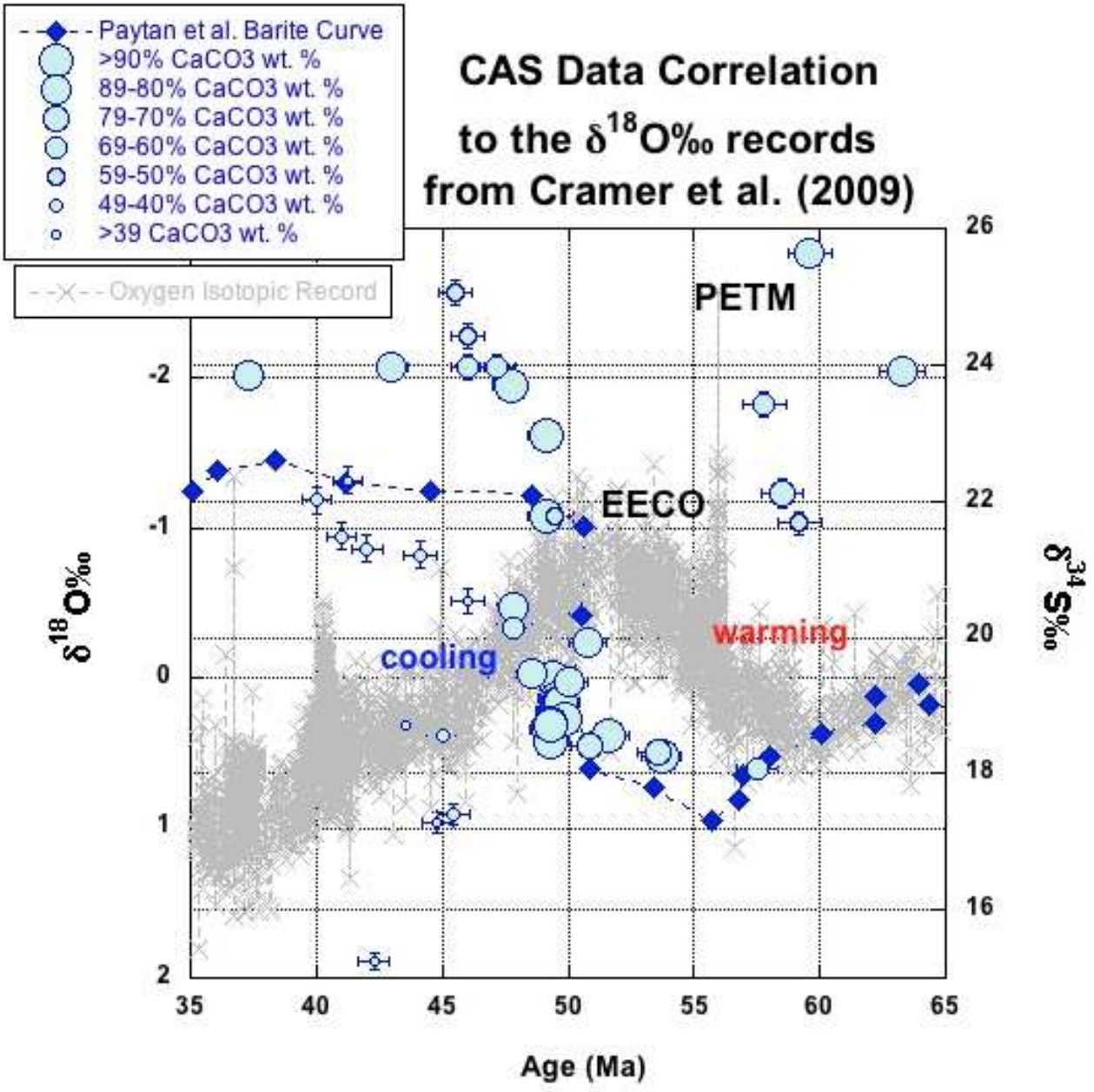

Figure 13: The binned CAS values and the $\delta^{18}O$ curve: *Bulk carbonate CAS $\delta^{34}S$ results from IODP and ODP samples are binned according to $CaCO_3$ wt. % and plotted in comparison to the Paytan et al. (1998) marine barite curve and the $\delta^{18}O$ curve compilation from Cramer et al. (2009) benthic foraminifera and adjusted to the 2012 Geologic Time Scale by Kristy Edgar and Pincelli Hull.*

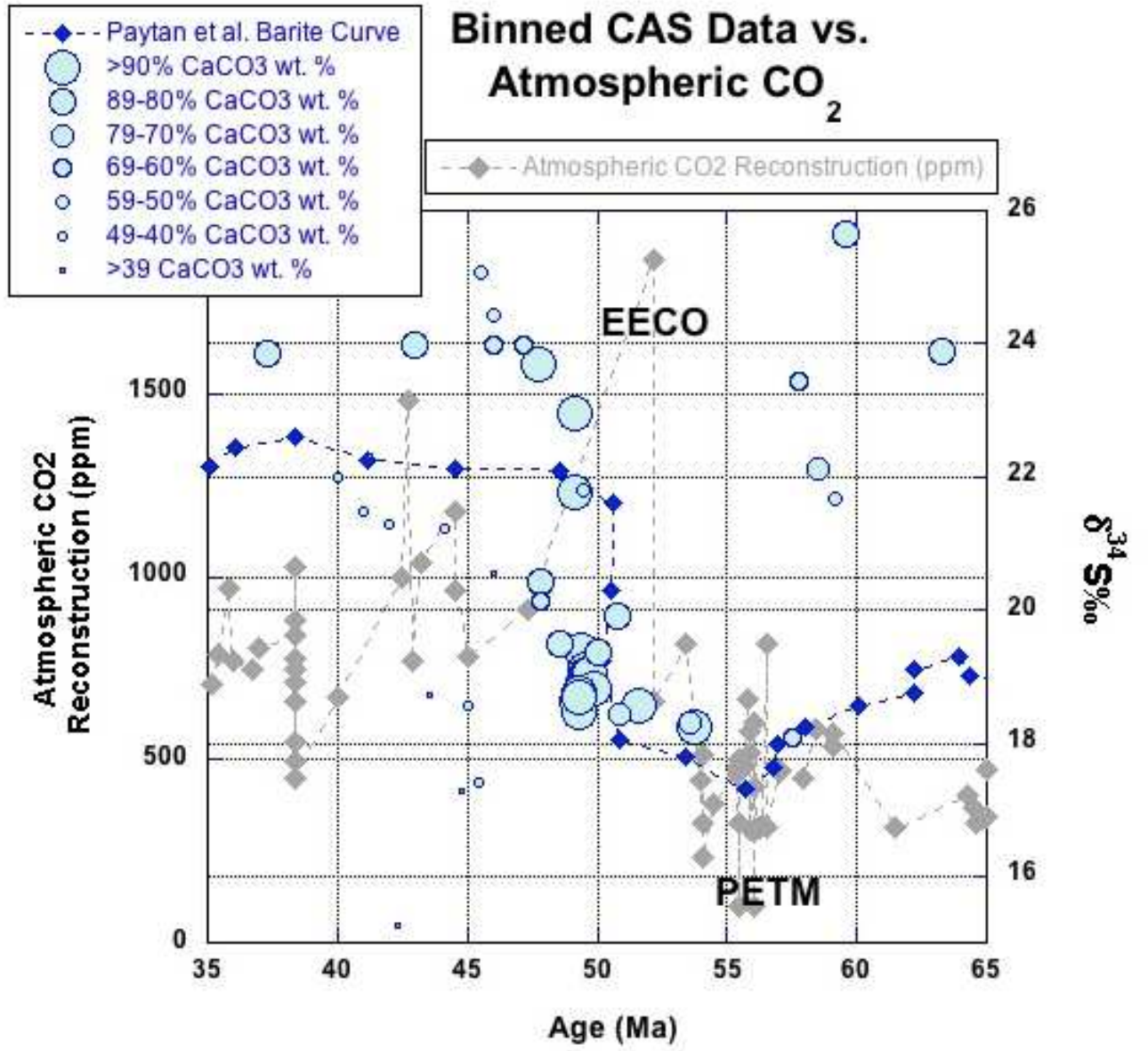

Figure 14: The binned CAS values and reconstructions of CO_2: *Bulk carbonate CAS $\delta^{34}S$ results from IODP and ODP samples are binned according to $CaCO_3$ wt. % and plotted in comparison to the Paytan et al. (1998) marine barite. Atmospheric CO2 reconstructions are compiled in Beerling and Royer (2011) and include data from Pagani et al., (2005), Doria et al.,(2011), Freeman and Hayes (1992), McElwain (1998), Smith et al.(2010), Royer et al., (2001), Stott (1992), Nordt et al., (2002), Beerling et al., (2002).*

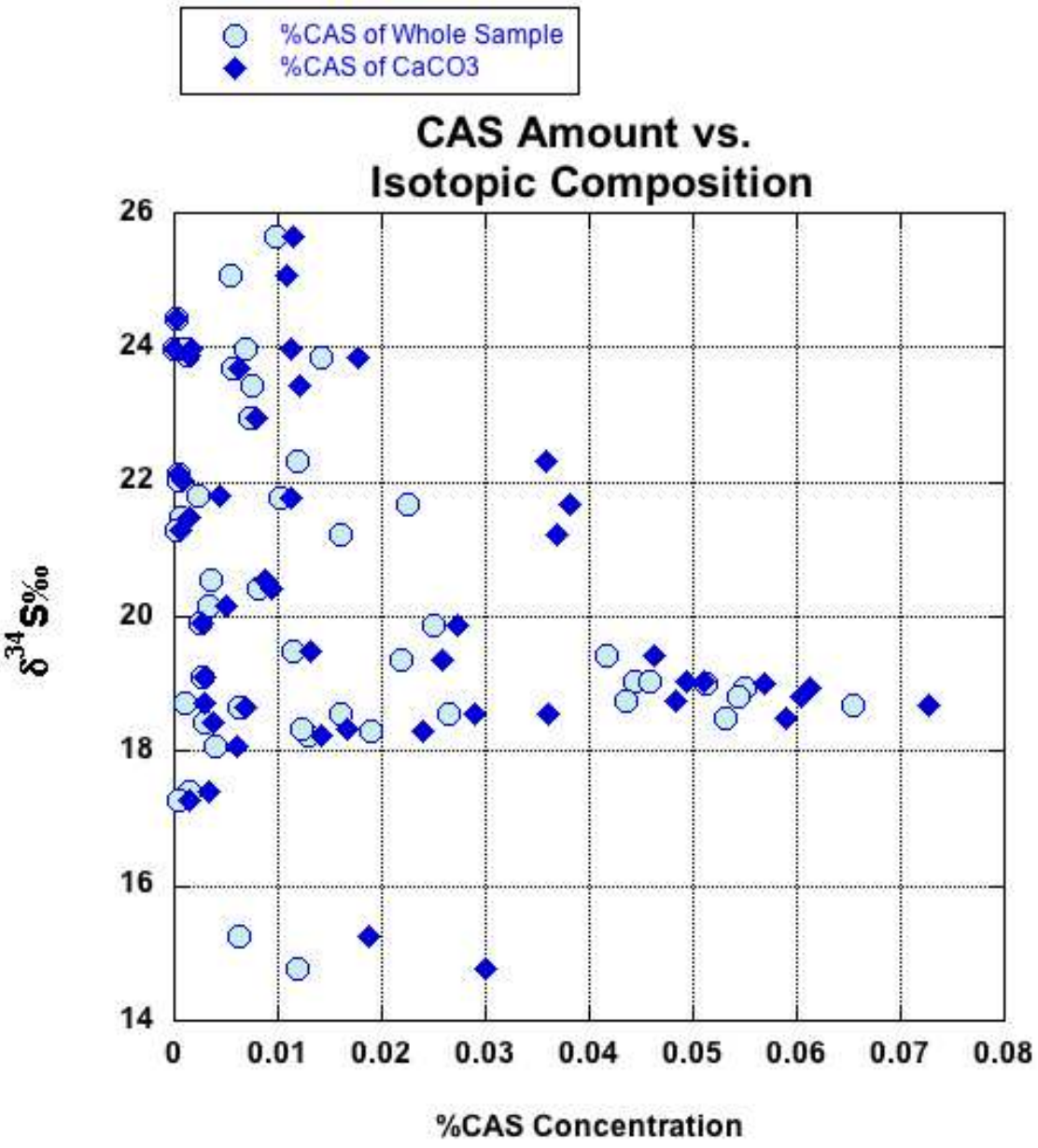

Figure 15: CAS $\delta^{34}S$ results corresponding to the amount of CAS (BaSO4): There appears to be more variability *$\delta^{34}S$ values associated with lower CAS concentrations. CAS has higher concentrations in samples with higher amounts of carbonate.*

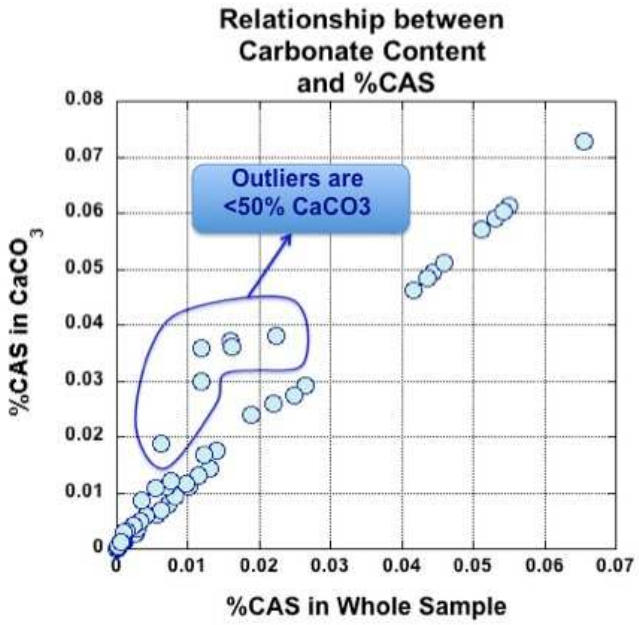

Figure 16: Comparison of %CAS in $CaCO_3$ vs. whole sample*: There is a positive correlation between the amount of CAS in a sample and the amount of CAS carbonates, which indicates that the only sources of sulfate in these samples are CAS (except for the outliers, which may contain oxidized sulfides). Higher carbonate contents correlate with higher CAS concentrations.*

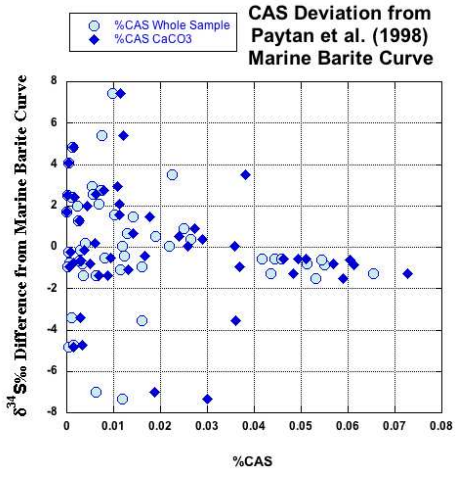

Figure 17: Variation from Marine Barite Curve: *The samples with a lower concentration of CAS exhibited a larger variation from the Paytan et al. (1998) marine barite curve than samples with higher CAS concentrations.*

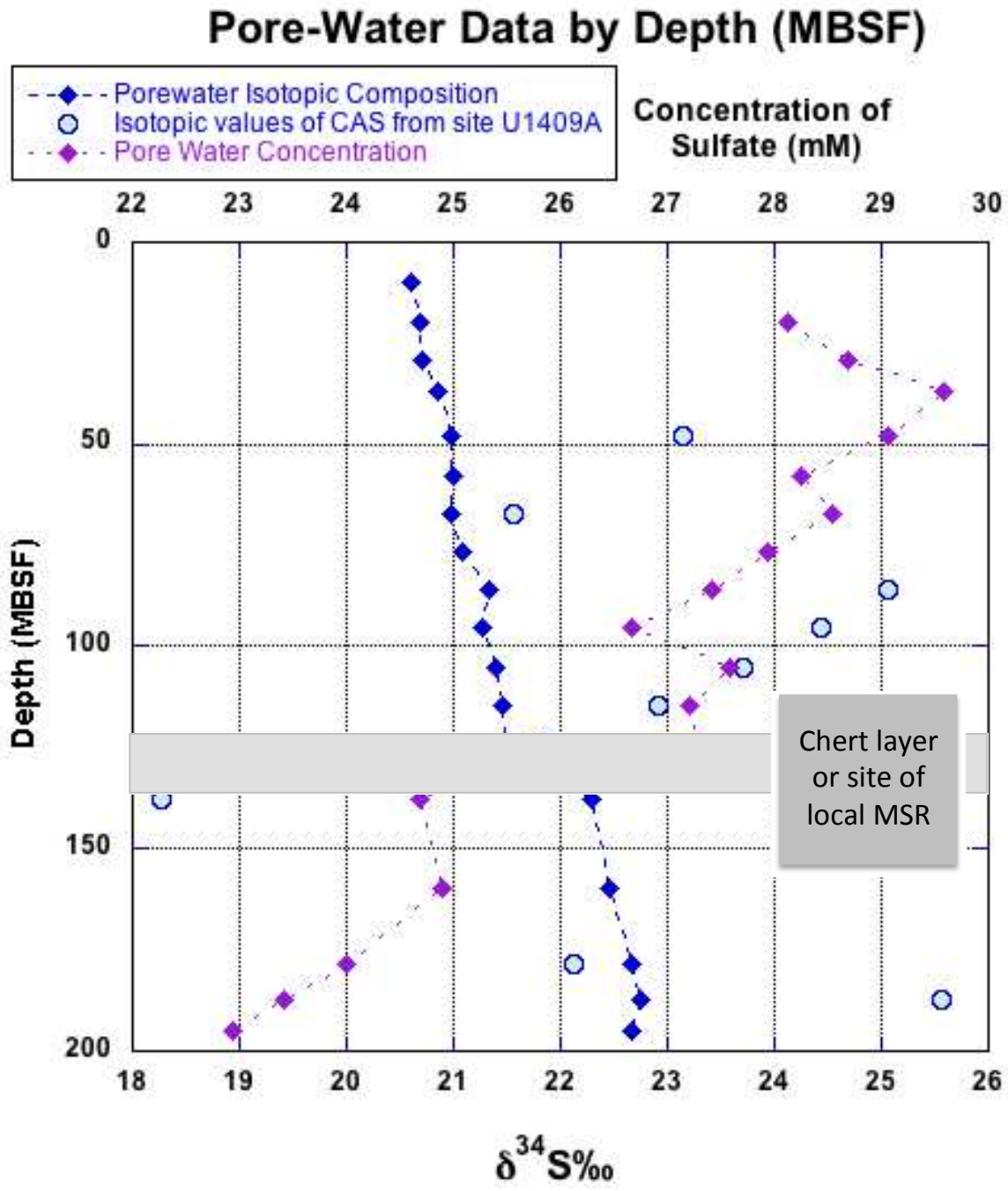

Figure 18: Pore-water Sulfate Values as a function of depth: *The $\delta^{34}S$ isotopic composition of pore water sulfates from squeeze cake samples from IODP site U1409A are plotted as a function of depth. As sulfate concentrations decrease, $\delta^{34}S$ values increase because MSR is actively occurring in the pore waters at depths of at least 200 mbsf.*

Table 1: Compilation of $\delta^{34}S$ CAS and Core values

Average $\delta^{34}S$‰	**Average Age based off of Bio and Chron**
18.55	51.64
23.7	47.70
21.78	49.11
18.24	53.70
18.93	49.45
19.41	49.38
22.96	49.10
19.86	70.14
18.64	49.20
18.48	49.34
19.11	49.51
19.00	49.58
19.03	49.65
19.05	49.72
18.81	49.85
18.74	49.34
18.7	49.27
20.43	47.84
19.48	48.57
19.36	50.05
25.65	59.60

23.85	37.3
23.97	43
23.90	63.25
19.92	50.78
18.31	53.54
22.12	58.5
18.42	50.87
18.34	96.16
23.97	47.2
18.08	57.54
20.15	47.84
23.98	46
23.43	57.8
21.79	49.47
24.43	46.01
25.06	45.49
21.68	59.2
22.01	40.03
21.3	42
17.4	45.43
21.49	41.02
21.21	44.12
18.57	45.02
15.25	42.28
14.76	45.49
22.31	41.25

18.71	43.53
17.29	44.81
20.54	46

Bibliography

Adams, D. D., Hurtgen, M. T., & Sageman, B. B. (2010). Volcanic triggering of a biogeochemical cascade during Oceanic Anoxic Event 2. *Nature Geoscience*, *3*(March), 3–6.

Arthur, M. (2000). Volcanic contributions to the carbon and sulfur geochemical cycles and global change. *Encyclopedia of Volcanoes*.

Ault, W. ., & Kulp, J. . (1959). Isotopic geochemistry of sulphur. *Geochimica et Cosmochimica Acta*.

Baublys, K. a., Golding, S. D., Young, E., & Kamber, B. S. (2004). Simultaneous determination of d33SV-CDT and d34SV-CDT using masses 48, 49 and 50 on a continuous flow isotope ratio mass spectrometer. *Rapid Communications in Mass Spectrometry*, *18*(22), 2765–2769.

Beerling, D. J., & Royer, D. L. (2011). Convergent Cenozoic CO2 history. *Nature Geoscience*.

Böttcher, M. E., Khim, B.-K., Suzuki, A., Gehre, M., Wortmann, U. G., & Brumsack, H.-J. (2004). Microbial sulfate reduction in deep sediments of the Southwest Pacific (ODP Leg 181, Sites 1119–1125): evidence from stable sulfur isotope fractionation and pore water modeling. *Marine Geology*, *205*(1-4), 249–260.

Bottrell, S. H., & Newton, R. J. (2006). Reconstruction of changes in global sulfur cycling from marine sulfate isotopes. *Earth-Science Reviews*, *75*(1-4), 59–83.

Bowles, M. W., Mogollón, J. M., Kasten, S., Zabel, M., & Hinrichs, K.-U. (2014). Global rates of marine sulfate reduction and implications for sub-sea-floor metabolic activities. *Science (New York, N.Y.)*, *344*(6186), 889–91.

Brinkhuis, H., Schouten, S., Collinson, M. E., Sluijs, A., Sinninghe Damsté, J. S., Dickens, G. R., … Moran, K. (2006). Episodic fresh surface waters in the Eocene Arctic Ocean. *Nature*, *441*(7093), 606–609. doi:10.1038/nature04692

Burdett, J., Arthur, M., & Richardson, M. (1989). A Neogene seawater sulfur isotope age curve from calcareous pelagic microfossils. *Earth and Planetary Science Letters*, *94*(3-4), 189–198. doi:10.1016/0012-821X(89)90138-6

Burke, K., & Sengor, a. M. C. (1988). Ten metre global sea-level change associated with South Atlantic Aptian salt deposition, *83*, 309–312. doi:10.1016/0025-3227(88)90064-3

Busenberg, E., & Plummer, L. N. (1985). Kinetic and thermodynamic factors controlling the distribution of SO32− and Na+ in calcites and selected aragonites. *Geochimica et Cosmochimica Acta*, *49*(3), 713–725.

Canfield, D. E. (2000). The Archean Sulfur Cycle and the Early History of Atmospheric Oxygen. *Science*, *288*(5466), 658–661.

Canfield, D. E. (2001). Isotope fractionation by natural populations of sulfate-reducing bacteria. *Geochimica et Cosmochimica Acta*.

Canfield, D. E. (2001). Isotope fractionation by natural populations of sulfate-reducing bacteria, *65*(7), 1117–1124.

Canfield, D. E. (2004). The Evolution of the Earth Surface Sulfur Reservoir. *Science (New York, N.Y.)*, *304*, 839–861.

Canfield, D. E., Farquhar, J., & Zerkle, A. L. (2010). High isotope fractionations during sulfate reduction in a low-sulfate euxinic ocean analog. *Geology*, *38*(5), 415–418.

Canfield, D. E., & Teske, A. (1996). Late Proterozoic rise in atmospheric oxygen concentration inferred from phylogenetic and sulfur-isotope studies. *Nature*, *382*(11), 127–132.

Caraco, N. F., Cole, J. J., & Likens, G. E. (1993). Sulfate control of phosphorus availability in lakes - A test and re-evaluation of Hasler and Einsele's model. *Hydrobiologia*, *253*(1-3), 275–280.

Carmody, B. R. W., Plummer, L. N., Busenberg, E., & Coplen, T. B. (1998). *Methods for collection of dissolved sulfate and sulfide and analysis of their sulfur isotopic composition*. *U.S. Geological Survey*.

Cather, S. M., Dunbar, N. W., McDowell, F. W., McIntosh, W. C., & Scholle, P. a. (2009). Climate forcing by iron fertilization from repeated ignimbrite eruptions: The icehouse-silicic large igneous province (SLIP) hypothesis. *Geosphere*, *5*(3), 315–324.

Claypool, G. (USGS), Holser, W. (University of O., Kaplan, I. (Universily of C., Sakai, H. (Okayama U., & Zak, I. (Hebrew U. (1980). The Age Curves of Sulfur and Oxygen Isotopes in Marine Sulfate and their Mutual Interpretation. *Chemical Geology*, *28*, 199–260.

Coplen, T. B., Brand, W. A., Gehre, M., Gro, M., Meijer, H. A. J., Toman, B., … Gmbh, U. F. Z. U. L. (2006). New Guidelines for δ 13 C Measurements. *Analytical Chemistry*, *78*(7), 2439–2441.

Cramer, B. S., Toggweiler, J. R., Wright, J. D., Katz, M. E., & Miller, K. G. (2009). Ocean overturning since the late cretaceous: Inferences from a new benthic foraminiferal isotope compilation. *Paleoceanography*, *24*(4).

Cui, Y., Kump, L. R., Ridgwell, A. J., Charles, A. J., Junium, C. K., Diefendorf, A. F., … Harding, I. C. (2011). Slow release of fossil carbon during the Palaeocene–Eocene Thermal Maximum, *4*(July), 481–485.

Dallanave, E., Agnini, C., Bachtadse, V., Muttoni, G., Crampton, J. S., Strong, C. P., … Slotnick, B. S. (2014). Early to middle Eocene magneto-biochronology of the southwest Pacific Ocean and climate influence on sedimentation: Insights from the Mead Stream section, New Zealand. *Geological Society of America Bulletin*, (X), 1–18.

Davydov, V. I., Korn, D., Schmitz, M. D., Gradstein, F. M., & Hammer, O. (2012). *The Geologic Time Scale*. *The Geologic Time Scale*.

Dickson, A. J., Rees-Owen, R. L., März, C., Coe, A. L., Cohen, A. S., Pancost, R. D., … Shcherbinina, E. (2014). The spread of marine anoxia on the northern Tethys margin during the Paleocene-Eocene Thermal Maximum. *Paleoceanography*, *29*(6), 471–488.

Epstein, S., & Mayeda, T. (1953). Variation of the 18O content of waters from natural sources. *Geochemica et Cosmochemica*, *4*, 213–224.

Erbacher, J., Mosher, D.C., Malone, M. . (2004). *Site 1258: Proceedings of the Ocean Drilling Program, Initial Reports Volume 207*. *Proceedings of the Ocean Drilling Program* (Vol. 207).

Erbacher, J., Mosher, D.C., Malone, M. J. (2004). *Leg 207 Summary: Proceedings of the Ocean Drilling Program, Initial Reports Volume 207*. *Proceedings of the Ocean Drilling Program* (Vol. 207).

Erbacher, J., Mosher, D.C., Malone, M. J. hipboar. S. (2004). *Site 1257: Proceedings of the Ocean Drilling Program, Initial Reports Volume 207*. *Proceedings of the Ocean Drilling Program* (Vol. 207).

Ganino, C., & Arndt, N. T. (2009). Climate changes caused by degassing of sediments during the emplacement of large igneous provinces. *Geology*, *37*(4), 323–326.

Gill, B. C., Lyons, T. W., & Frank, T. D. (2008). Behavior of carbonate-associated sulfate during meteoric diagenesis and implications for the sulfur isotope paleoproxy. *Geochimica et Cosmochimica Acta*, *72*, 4699–4711.

Gradstein, F. M., Ogg, J. G., & Hilgen, F. J. (2012). On The Geologic Time Scale. *Newsletters on Stratigraphy*.

Griffith, E. M., & Paytan, A. (2012). Barite in the ocean - occurrence, geochemistry and palaeoceanographic applications. *Sedimentology*, *59*(6), 1817–1835.

Habicht, K. S., Gade, M., Thamdrup, B., Berg, P., & Canfield, D. E. (2002). Calibration od Sulfate Levels in the Archean Ocean. *Science (New York, N.Y.)*, *298*, 2372–2374.

Hardie, L. A. (1996). Secular variation in seawater chemistry: An explanation for the coupled secular variation in the mineralogies of marine limestones and potash evaporites over the past 600 m.y. *Geology*, *24*, 279–283.

Harrison, T. M., Copeland, P., Kidd, W. S. F., & Yin, A. N. (1992). Raising Tibet. *Science*, *255*(March).

Hay, W. W., Migdisov, A., Balukhovsky, A. N., Wold, C. N., Flögel, S., & Söding, E. (2006). Evaporites and the salinity of the ocean during the Phanerozoic: Implications for climate, ocean circulation and life. *Palaeogeography, Palaeoclimatology, Palaeoecology*, *240*(1-2), 3–46.

Henrichs, S. M., & Reeburgh, W. S. (1987). Anaerobic mineralization of marine sediment organic matter: Rates and the role of anaerobic processes in the oceanic carbon economy. *Geomicrobiology Journal*.

Higgins, J. A., & Schrag, D. P. (2006). Beyond methane: Towards a theory for the Paleocene-Eocene Thermal Maximum. *Earth and Planetary Science Letters*, *245*(3-4), 523–537.

Horita, J., Zimmermann, H., & Holland, H. D. (2002). Chemical evolution of seawater during the Phanerozoic. *Geochimica et Cosmochimica Acta*, *66*(21), 3733–3756.

Hurtgen, M. T., Arthur, M. a., Suits, N. S., & Kaufman, A. J. (2002). The sulfur isotopic composition of Neoproterozoic seawater sulfate: implications for a snowball Earth? *Earth and Planetary Science Letters*, *203*(1), 413–429.

Kah, L. C., Lyons, T. W., & Frank, T. D. (2004). Low marine sulphate and protracted oxygenation of the Proterozoic biosphere. *Nature*, *431*(7010), 834–8.

Kaiho, K. (1991). Global changes of Paleogene aerobic/anaerobic benthic foraminifera and deep-sea circulation. *Palaeogeography, Palaeoclimatology, Palaeoecology*, *83*(1-3), 65–85.

Kampschulte, A., & Strauss, H. (2004). The sulfur isotopic evolution of Phanerozoic seawater based on the analysis of structurally substituted sulfate in carbonates. *Chemical Geology*, *204*(3-4), 255–286.

Kao, S. J., Hsu, S. C., Horng, C. S., & Liu, K. K. (2004). Carbon-sulfur-iron relationships in the rapidly accumulating marine sediments off southwestern Taiwan. *Geochemical Society Special Publications*, *9*(C), 441–457.

Kaplan, I. R., Emery, K. O., & Rittenbebg, S. C. (1963). The distribution and isotopic abundance of sulphur in recent marine sediments off southern California. *Geochimica et Cosmochimica Acta*.

Kasten, S., & Jørgensen, B. B. (2000). Sulfate reduction in marine sediments. In *Marine Geochemistry* (pp. 263–282).

Kump, L. R., & Arthur, M. A. (1999). Interpreting carbon-isotope excursions: carbonates and organic matter. *Chemical Geology*.

Kurtz, a. C., Kump, L. R., Arthur, M. a., Zachos, J. C., & Paytan, A. (2003). Early Cenozoic decoupling of the global carbon and sulfur cycles. *Paleoceanography*, *18*(4), 1–14.

Larson, R. L. (1991). Geological consequences of superplumes. *Geology*. 963-966

Lowenstein, T. K., & Demicco, R. V. (2006). Elevated Eocene atmospheric CO2 and its subsequent decline. *Science (New York, N.Y.)*, *313*(5795), 1928.

Lowenstein, T. K., Hardie, L. A., Timofeeff, M. N., & Demicco, R. V. (2003). Secular variation in seawater chemistry and the origin of calcium chloride basinal brines. *Geology*, *31*(10), 857–860.

Lowenstein, T. K., Timofeeff, M. N., Brennan, S. T., Hardie, L. A., & Demiccol, R. V. (2001). Oscillations in Phanerozoic Seawater Chemistry : Evidence from FLuid IncLusions. *Science*, *294*, 10866–1088.

Lyons, T. W., Gellatly, A. M., McGoldrick, P. J., & Kah, L. C. (2006). Proterozoic sedimentary exhalative (SEDEX) deposits and links to evolving global ocean chemistry. *Geologic Society of America*, *Memoir 198*, 169–184.

Lyons, T. W., Walter, L. M., Gellatly, A. M., Martini, A. M., & Blake, R. E. (2004). Sites of anomalous organic remineralization in the carbonate sediments of South Florida, USA: The sulfur cycle and carbonate-associated sulfate. *Geological Society of America Special Papers*, *379*, 161–176.

Marenco, P. J., Corsetti, F. a., Kaufman, A. J., & Bottjer, D. J. (2008). Environmental and diagenetic variations in carbonate associated sulfate: An investigation of CAS in the Lower Triassic of the western USA. *Geochimica et Cosmochimica Acta*, *72*(6), 1570–1582.

Mazumdar, A., Goldberg, T., & Strauss, H. (2008). Abiotic oxidation of pyrite by Fe (III) in acidic media and its implications for sulfur isotope measurements of lattice-bound sulfate in sediments. *Chemical Geology*, *253*, 30–37.

Miller, K. G., Browning, J. V, Pekar, S. F., & Sugarman, P. J. (1997). Cenozoic evolution of the new jersey coastal plain: changes in sea level, tectonics, and sediment supply 1. *Proceedings of the Ocean Drilling Program, Scientific Results*, *150*, 361–373.

Molnar, P., & Tapponnier, P. (1975). Cenozoic Tectonics of Asia : Effects of a Continental Collision. *Science*, *189*(4201), 419–426.

Norris, R. D., Wilson, P. A., Blum, P., Fehr, A., Agnini, C., Bornemann, A., … Yamamoto, Y. (2014a). *Site U1406: Proceedings of the Integrated Ocean Drilling Program, Volume 342*. *Proceedings of the Integrated Ocean Drilling Program* (Vol. 342).

Norris, R. D., Wilson, P. A., Blum, P., Fehr, A., Agnini, C., Bornemann, A., … Yamamoto, Y. (2014b). *Site U1407: Proceedings of the Integrated Ocean Drilling Program, Volume 342*. *Proceedings of the Integrated Ocean Drilling Program* (Vol. 342).

Norris, R. D., Wilson, P. A., Blum, P., Fehr, A., Agnini, C., Bornemann, A., … Yamamoto, Y. (2014c). *Site U1408: Proceedings of the Integrated Ocean Drilling Program, Volume 342*. *Proceedings of the Integrated Ocean Drilling Program* (Vol. 342).

Norris, R. D., Wilson, P. A., Blum, P., Fehr, A., Agnini, C., Bornemann, A., … Yamamoto, Y. (2014d). *Site U1409: Proceedings of the Integrated Ocean Drilling Program, Volume 342*. *Proceedings of the Integrated Ocean Drilling Program* (Vol. 342).

Norris, R. D., Wilson, P. A., Blum, P., Fehr, A., Agnini, C., Bornemann, A., … Yamamoto, Y. (2014e). *Site U1410: Proceedings of the Integrated Ocean Drilling Program, Volume 342*. *Proceedings of the Integrated Ocean Drilling Program* (Vol. 342).

Ohkouchi, N., Kawamura, K., Kajiwara, Y., Wada, E., Okada, M., Kanamatsu, T., & Taira, a. (1999). Sulfur isotope records around Livello Bonarelli (northern Apennines, Italy) black shale at the Cenomanian-Turonian boundary. *Geology*, *27*, 535–538.

Pagani, M., Pedentchouk, N., Huber, M., Sluijs, A., Schouten, S., Brinkhuis, H., … Dickens, G. R. (2006). Arctic hydrology during global warming at the Palaeocene/Eocene thermal maximum. *Nature*, *442*(7103), 671–675.

Patriat, P., & Achache, J. (1984). India-Eurasia Collision Chronology has Implications for Crustal Shortening and Driving Mechanism of Plates. *Nature*, *311*(18), 615–621.

Paytan, A., & Gray, E. T. (2012). Sulfur Isotope Stratigraphy. In *The Geologic Time Scale* (Vol. The Geolog, pp. 167–180).

Paytan, A., Ivy, A., & Wankel, S. D. (2004). Using sulfur isotopes to elucidate the origin of barite associated with high organic matter accumulation events in marine sediments. *Geological Society of America Special Paper 379*, *spe379-10*, 151–160.

Paytan, A., Kastner, M., Campbell, D., & Thiemens, M. (1998). Sulfur isotopic composition of cenozoic seawater sulfate. *Science (New York, N.Y.)*, *282*(5393), 1459–62.

Paytan, A., Kastner, M., Campbell, D., & Thiemens, M. H. (2004a). Seawater sulfur isotope fluctuations in the Cretaceous. *Science (New York, N.Y.)*, *304*, 1663–1665.

Paytan, A., Kastner, M., Campbell, D., & Thiemens, M. H. (2004b). Seawater sulfur isotope fluctuations in the Cretaceous. *Science (New York, N.Y.)*, *304*, 1663–1665.

Paytan, A., Mearon, S., Cobb, K., & Kastner, M. (2002). Origin of marine barite deposits: Sr and S isotope characterization. *Geology*, *30*(8), 747–750.

Pingitore, N., Meitzner, G., & Love, K. (1995). Identification of sulfate in natural carbonates by X-ray absorption spectroscopy. *Geochimica et Cosmochimica Acta*, *59*, 2477–2483.

Raab, M., & Spiro, B. (1991). Sulfur Isotopic Variations during seawater evaporation with fractional crystalization. *Chemical Geology: Isotope Geoscience Section*, *86*(4), 323–333.

Raymo, & Ruddiman. (1992). Tectonic forcing of late Cenozoic climate. *Nature*, *359*, 117–122.

Rees, C. E., Jenkins, W. J., & Monster, J. (1978). The sulphur isotopic composition of ocean water sulphate. *Geochimica et Cosmochimica Acta*, *42*(4), 377–381.

Rennie, V. C. F., & Turchyn, A. V. (2014). The preservation of d34S-SO4 and d18O-SO4 in carbonate-associated sulfate during marine diagenesis: A 25 Myr test case using marine sediments. *Earth and Planetary Science Letters*, *395*, 13–23.

Riccardi, A. L. (2007). *Carbonate-Associated Sulfate: Assessment of and use as an Isotopic Proxy for Global Sulfur Cycling During End-Permian Mass Extinction*. Penn State University Dissertation

Richter, F. M., Rowley, D. B., & DePaolo, D. J. (1992). Sr isotope evolution of seawater: the role of tectonics. *Earth and Planetary Science Letters*, *109*(1-2), 11–23.

Self, S., Blake, S., Sharma, K., Widdowson, M., & Sephton, S. (2008). Sulfur and Chlorine in Late Cretaceous. *Science*, *319*(March), 1654–1657.

Sexton, P. F., Norris, R. D., Wilson, P. a, Pälike, H., Westerhold, T., Röhl, U., … Gibbs, S. (2011). Eocene global warming events driven by ventilation of oceanic dissolved organic carbon. *Nature*, *471*(7338), 349–352.

Stein, R., Boucsein, B., & Meyer, H. (2006). Anoxia and high primary production in the Paleogene central Arctic Ocean: First detailed records from Lomonosov Ridge. *Geophysical Research Letters*, *33*(18), 1–6.

Storey, M., Duncan, R. A., & Swisher, C. C. (2007). Paleocene-Eocene thermal maximum and the opening of the Northeast Atlantic. *Science (New York, N.Y.)*, *316*(5824), 587–589.

Strauss, H. (1997). The isotopic composition of sedimentary sulfur through time. *Palaeo*, *132*, 97–118.

Strauss, H. (1999). Geological evolution from isotope proxy signals — sulfur. *Chemical Geology*.

Thode, H. G., & Monster, J. (1961). Sulphur isotope geochemistry. *Geochimica et Cosmochimica Acta*, *25*(1950), 159–174.

Timofee, M. N., Lowenstein, T. K., Augusta, M., & Harris, N. B. (2006). Secular variation in the major-ion chemistry of seawater : Evidence from fluid inclusions in Cretaceous halites. *Geochimica et Cosmochimica Acta*, *70*, 1977–1994. 0

Turchyn, A. V, & Schrag, D. P. (2004). Oxygen isotope constraints on the sulfur cycle over the past 10 million years. *Science (New York, N.Y.)*, *303*, 2004–2007.

Turchyn, A. V, & Schrag, D. P. (2006). Cenozoic evolution of the sulfur cycle: Insight from oxygen isotopes in marine sulfate. *Earth and Planetary Science Letters*, *241*, 763–779.

Turchyn, A. V., Schrag, D. P., Coccioni, R., & Montanari, A. (2009). Stable isotope analysis of the Cretaceous sulfur cycle. *Earth and Planetary Science Letters*, *285*, 115–123.

Walker, J. C. (1986). Global geochemical cycles of carbon, sulfur and oxygen. *Marine Geology*, *70*, 159–174.

Wieser, M. E. (2006). Atomic weights of the Elements 2005. *Journal of Physical and Chemical Reference Data*, *36*, 485–496.

Wortmann, U. G., Chernyavsky, B., Bernasconi, S. M., Brunner, B., Böttcher, M. E., & Swart, P. K. (2007). Oxygen isotope biogeochemistry of pore water sulfate in the deep biosphere: Dominance of isotope exchange reactions with ambient water during microbial sulfate reduction (ODP Site 1130). *Geochimica et Cosmochimica Acta*, *71*(17), 4221–4232.

Wortmann, U. G., & Paytan, A. (2012). Rapid variability of seawater chemistry over the past 130 million years. *Science (New York, N.Y.)*, *337*(6092), 334–336.

Wotte, T., Shields-zhou, G. A., & Strauss, H. (2012). Carbonate-associated sulfate : Experimental comparisons of common extraction methods and recommendations toward a standard analytical protocol. *Chemical Geology*, *327*, 132–144.

Wu, S., Bally, A. W., & Cramez, C. (1990). Allochthonous salt, structure and stratigraphy of the north-eastern Gulf of Mexico. Part II: Structure. *Marine and Petroleum Geology*, *7*(4), 334–370.

Zachos, J. C., Dickens, G. R., & Zeebe, R. E. (2008). An early Cenozoic perspective on greenhouse warming and carbon-cycle dynamics. *Nature*, *451*(7176), 279–283.

Vita: Kara Dennis

1396 Bayard Ave. • St. Paul, MN 55116
612-670-1960 • kedennis@syr.edu

Education

M.S. **Earth Sciences, Syracuse University** (May 2015), THESIS: *"Using the Sulfur Cycle to Constrain Changes in Seawater Chemistry During the Paleogene*" Under the supervision of Christopher Junium

B.A. **Geology, Macalester College** (May 2012), THESIS: *"Regional Climate Change and Geomorphic History of Grinnell Glacier in Glacier National Park, MT"* Under the supervision of Kelly MacGregor

Research Experience

- Research Assistant and Lamont-Doherty Earth Observatory at Columbia University in the Core Repository — Jan 2015- present
- CAS (carbonate-associated sulfate) extraction and pore-water sulfate extraction from IODP core samples — Fall 2013- present
- Sample Prep and Analysis on Isoprime coupled EA-IRMS (mostly sulfur isotopic analysis) — Summer 2013-present
- Petrologic and geochemical analysis of Paleoproterozoic rocks of the Penokean orogeny (Central MN) — Spring 2012
- Oceanographic field research: Ocean and Climate, SEA Semester (Boston University and Woods Hole Oceanographic Institute) — Summer and Fall 2010
- Hydrologic Field Research: Hydrology Field Camp, University of Minnesota

Awards

- Chair Award, *Syracuse University Earth Sciences* ($300) — Spring 2014
- GSA Graduate Student Grant ($900) — Summer 2014

Teaching Experience (Syracuse University: Earth Science and Science Teaching Departments)

- Teaching Assistant Coordinator for Oceanography and Earthquakes and Volcanoes — Fall 2013 and Spring 2014
- Teaching Assistant for Oceanography — Fall 2012 &2014,Spring2013
- Graduate Assistant for Frontiers of Science Program, which provides the opportunity for high school students to learn about different fields of science through lectures and activities — Fall 2012-present

- Lava MOOC, Helping with the construction of an online course for the Syracuse University Lava Project — Spring and Summer 2014

Professional Development

- Waggoner Geology Seminar coordinator, *Syracuse University*, schedule student speakers and publicity — Fall 2012-Spring 2014
- Geology Club Webmaster, *Syracuse University*, maintaining website and planning field trips (Spring Break trips 2013 & 2014) — Summer 20013-Spring 2014
- Senior Resident Advisor, *Macalester College*, responsible for implementing CLM curriculum within the dormitory and peer leader for other RAs and organizing staff meetings — Fall 2009- May 2012
- Senior Class Gift Planning Committee, *Macalester College*, fundraising and event planning — September 2011-May 2012
- Leasing Consultant, *Quadrangle Development Corp*., drafting leases, sales experience, and event planning — Summer 2011

Research Interests

- Changes in seawater chemistry over geologic time, with an emphasis on the biogeochemical cycling of sulfur and its relation to the carbon and oxygen cycles.
- The implication of massive evaporite weathering/precipitation on seawater chemistry
- Earth science education and scientific literacy, communication and outreach

Research Skills

- Instrumentation: Coupled Isoprime EA-IRMS, XRD, SEM, Carbon Coulometer
- Software: Arc-GIS, MATLAB, R, ODV (Ocean Data View)

Publications/Presentations

- Kara Dennis and Christopher Junium. Interrogating the Paleogene sulfur cycle, carbonate-associated sulfate and pore water sulfate $d^{34}S$ from Demerara Rise and Newfoundland Drifts. Poster PP51B-1126 AGU 2015